HISTORICAL BIOLOGY
https://doi.org/10.1080/08912963.2018.1539970

Taylor & Francis
Taylor & Francis Group

ARTICLE

Redescription of the cervical vertebrae of the Mamenchisaurid Sauropod *Xinjiangtitan shanshanesis* Wu et al. 2013

Xiao-Qin Zhang[a,b], Da-Qing Li[a,c], Yan Xie[d] and Hai-Lu You[e,f,g]

[a]School of Earth Sciences and Resources, China University of Geosciences (Beijing), Beijing, P. R. China; [b]Gansu Geological Museum, Lanzhou, P. R. China; [c]Institute of Vertebrate Paleontology and College of Life Science and Technology, Gansu Agricultural University, Lanzhou, P. R. China; [d]Center of Conservation and Research of fossils in Shanshan, Bureau of Land and Resources of Shanshan County, Xinjiang Uygur Autonomous Region, P. R. China; [e]Key Laboratory of Vertebrate Evolution and Human Origins, Institute of Vertebrate Paleontology and Paleoanthropology, Chinese Academy of Sciences, Beijing, P. R. China; [f]CAS Center for Excellence in Life and Paleoenvironment, Beijing, P. R. China; [g]University of Chinese Academy of Sciences, Beijing, P. R. China

ABSTRACT

Xinjiangtitan shanshanesis was originally reported based on the last two cervical vertebrae, complete dorsal and sacral vertebrae, two anterior caudal vertebrae, a partial pelvic girdle and partial hind limb bones from one individual specimen. However, the original description was brief and problematic. The ongoing excavation and further preparation of the holotype have revealed a complete cervical vertebral series. Herein, we provide a full redescription of the old and new materials of the cervical column of *Xinjiangtitan shanshanesis* and revised the diagnostic features of this taxon.

ARTICLE HISTORY
Received 7 June 2018
Accepted 17 October 2018

KEYWORDS
Xinjiangtitan shanshanesis; Mamenchisauridae; Sauropod; Late Jurassic; cervical vertebrae; anatomy

Introduction

The Jurassic terrestrial sediments are well developed in Xinjiang, northwestern China, and abundant sauropod fossils have been yielded from this region. *Tienshanosaurus chitaiensis* was reported from the Oxfordian (Upper Jurassic) Shishugou Formation of Qitai in the northern Xinjiang (Young, 1937). Though Sekiya (2011) has assigned it to Mamenchisauridae, the affinity of *Tienshanosaurus* is controversial due to fragmentary of the materials and a limited original description. *Chiayusaurus lacustris* was discovered in the Late Jurassic strata in the Turpan Basin (Bohlin, 1953; Li 1998). *Klameilisaurus gobiensis* was excavated from the Middle Jurassic Wucaiwan Formation in the Jiangjunmiao Region in 1984 by the Institute of Vertebrate Paleontology and Paleoanthropology (IVPP) field crew (Zhao 1993; Li 1998). *Bellusaurus sui*, a small sauropod, was discovered and reported from the Middle-Late Jurassic Wucaiwan and Shishugou Formations in Jiangjunmiao and Karamay regions (Dong, 1990). *Mamenchisaurus sinocanadorum* was reported from the Late Jurassic Shishugou Formation in the eastern Junggar Basin (Russell and Zheng 1993). *Hudiesaurus sinojapanorum* was discovered from the Kalazha Formation of Shanshan County of the Turpan Basin (Dong, 1997; Xu et al., 2014).

In 2012, a joint research team of Jilin University, Shenyang Normal University and Xinjiang Geological Survey Institute discovered *Xinjiangtitan shanshanesis* in a quarry 8 km south to Qiketai (Figure 1). The type specimen (**SSV**12001) was discovered from the Qigu Formation which is underlying the Kalazha Formation and the exposed bones included two posterior cervical vertebrae, complete dorsal vertebrae and sacral vertebrae, two anterior caudal vertebrae, a partial pelvic girdle and partial hind limbs. However, other parts of the skeleton were unexposed and left unexcavated in the rocks at that time. Therefore, the initial description of *Xinjiangtitan shanshanesis* (Wu et al. 2013) is limited, and the authors mistook the last cervical vertebra as the first dorsal vertebra and misidentified the 10th and 11th dorsal vertebrae as a single dorsal vertebra.

From September 2014 to June 2015, the government of Shanshan County organized another excavation for the same specimen and found the complete and articulated vertebral column of **SSV**12001, including 18 cervical vertebrae, 12 dorsal vertebrae, 5 sacral vertebrae and 39 caudal vertebrae (it is estimated that only the last two caudal vertebrae are lost).

The vertebral morphology is critical in understanding the sauropod evolution (Harris 2006). *Xinjiangtitan shanshanesis* preserves the most complete vertebral column of all sauropods ever found in Xinjiang, and probably also so in Asia. Here we provide a detailed description on the cervical vertebrae of *Xinjiangtitan shanshanesis* and revise the diagnostic features of the cervical series of this taxon.

Institutional abbreviations

SSV, Shanshan Geological Museum, Shanshan.

Anatomical abbreviations

acdl (ACDL), anterior centrodiapophyseal lamina; a.lpf (A.LPF), anterior longitudinal pneumatic fossa; a.f, articular surface for odontoid process; a.s, articular surface for axis; at.

CONTACT Da-Qing Li daqingli@gsau.edu.cn Institute of Vertebrate Paleontology and College of Life Science and Technology, Gansu Agricultural University, Lanzhou, 730070, P. R. China

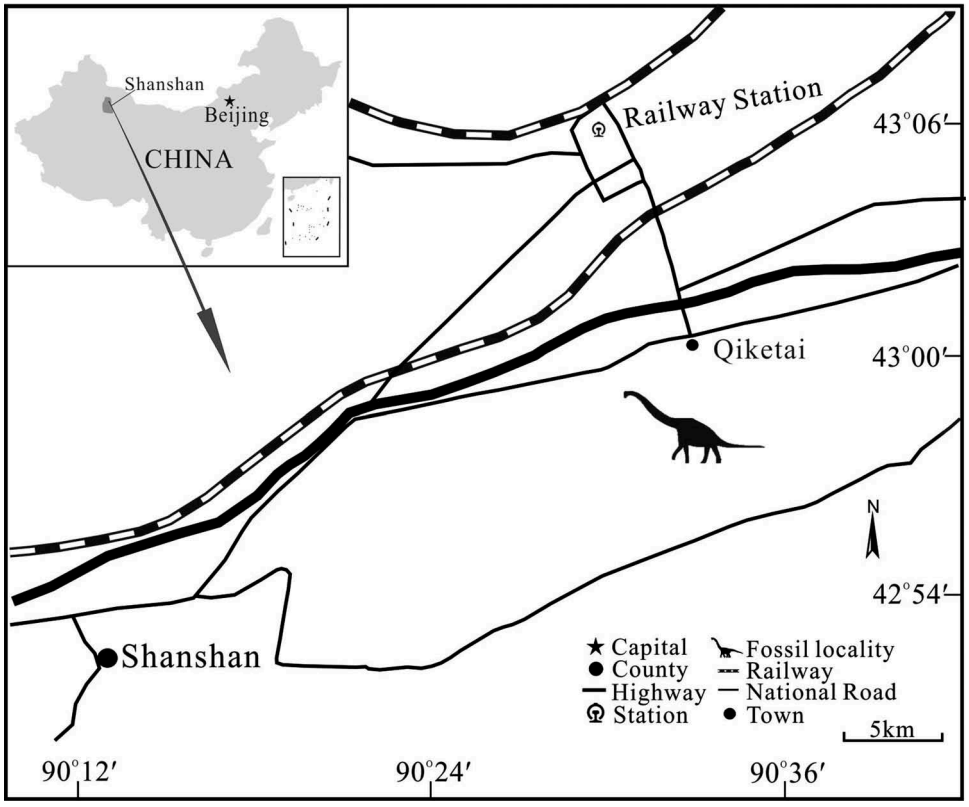

Figure 1. Location of *Xinjiangtitan shanshanesis* (SSV120001).

ic, atlantal intercentrum; Ca, caudal; cap, capitulunm; cdf (CDF), centrodiapophyseal fossa; Ch,chevron; cpof (CPOF), centropostzygapophyseal fossa; cpol (CPOL), centropostzygapophyseal lamina; cprf (CPRF), centroprezygapophyseal fossa; cprl (CPRL), centroprezygapophyseal lamina; Cv, cervical vertebra; D, dorsal vertebra; d, odontoid process; di, diapophysis; epi, epipophysis; f, fossa; fo, foramen; h.ri, horizontal ridge; ic, intercentrum; Ish, ischium; k, keel; lpf (LPF), longitudinal pneumatic fossa; L.fe, left femur; L.mt, left metatarsal; L.ti, left tibia; mp, metapophyses; mt, median tubercle; n.c, neural canal; np, neuropophysis; o.ri, oblique ridge; pa, parapophysis; pcdl, posterior centrodiapophyseal lamina; pl, pleurocoel; p.lpf (P.LPF), posterior longitudinal pneumatic fossa; pn, pneumatopre; pocdf (POCDF), postzygapophyseal centrodiapophyseal fossa; podl (PODL), postzygodiapophyseal lamina; poz, postzygapophysis; prcdf (PRCDF), prezygapophyseal centrodiapophyseal fossa; prdl (PRDL), prezygodiapophyseal lamina; prz, prezygapophysis; Pu, pubis; ri, ridge; S, sacral vertebrae; sdf (SDF), spinodiapophyseal fossa; sp, neural spine; spdl (SPDL), spinodiapophyseal lamina; spof (SPOF), spinopostzygapophyseal fossa; spol (SPOL), spinopostzygapophyseal lamina; sprf (SPRF), spinoprezygapophyseal fossa; sprl (SPRL), spinoprezygapophyseal lamina; tlp, triangular lateral process; tprl (TPRL), intraprezygapophyseal lamina; tpol (TPOL), intrapostzygapophyseal lamina; tub, tuberculum; Ung, ungual; v.f, ventral fossa; v.k, ventral keel; vlr, ventrolateral ridge. Nomenclature and abbreviation for vertebral laminae and fossae are following Wilson (1999), Wilson and Upchurch (2009), Wilson et al. (2011) and Wilson (2012).

Systematic palaeontology

Dinosauria Owen, 1842
Saurischia Seeley, 1887
Sauropoda Marsh, 1878
Mamenchisauridae Yang & Zhao, 1972
Xinjiangtitan Wu et al., 2013
Xinjiangtitan shanshanesis Wu et al., 2013

Holotype

The original materials of the holotype (**SSV**12001, Wu et al. 2013) include the last two cervical vertebrae, 12 dorsal vertebrae, 5 sacral vertebrae, the first two caudal vertebrae, both pubes, the left ischium, the left femur, the left tibia, the left fibula, a metatarsal and some fragmentary cervical and dorsal ribs. With new materials recovered, the **SSV**12001 now includes a partial cranium, 18 complete cervical vertebrae, 12 almost complete dorsal vertebrae excluding the ventral portion of the centra of dorsal vertebra 1–9, 5 articulated sacral vertebrae, 39 caudal vertebrae, partial cervical and dorsal ribs, 18 chevrons, the left ilum, both pubes, both ischia, the left femur, the left tibia, the left fibula, the left astragalus, and a partial left pes. The type specimen is hosted in the Shanshan Geological Museum, Shanshan.

Locality and horizon

The quarry is located 30 km east to Shanshan, and 8 km south to Qiketai (Figure 1). Wu et al. (2013) considered that the

fossil bed was from the Qigu Formation, which is early Late Jurassic based (Deng et al. 2015).

Revised Diagnosis

A mamenchisaurid dinosaur with the following unique combination of characters: (1) ventral keel extending almost along the middle-posterior portion of the ventral surface in Cv 3–12 but confined to the anterior concavity in Cv 13–17*; (2) longest cervical is Cv 12* (vs. Cv 14 in *Mamenchisaurus youngi*; Cv 11–12 in *Mamenchisaurus hochuanensis*; Cv 15 in *Qijianglong guokr*); (3) the ratio of the length of Cv 3: Cv 2 is 1.58* (vs. 1.37 in *Mamenchisaurus youngi*; 1.34 in *Mamenchisaurus hochuanensis*; 1.79 in *Qijianglong guokr*; 1.7 in *Mamenchisaurus sinocanadorum*); (4) lateral longitudinal pleurocoel divided by an anterodorsally oblique ridge into the anterior and posterior parts (similar to *Mamenchisaurus youngi*); (5) horizontal ridge present dorsal to the lateral pneumatic fossa of the last two cervical centra*; (6) subtle keel (incipient epipophyseal-prezygapophyseal lamina) subdividing spinodiapophyseal fossa in Cv 9–18 (present in Cv 16–17 of *Qijianglong guokr*); (7) pneumatopores in spinodiapophyseal fossa in the middle-posterior cervical vertebrae (similar to *Qijianglong guokr*); (8) only the last cervical neural spine bifurcated with the median tubercle*.(characters with an asterisk represents autapomorphies of *Xinjiangtitan shanshanesis*)

Description

In **SSV**12001, the cervical series is almost completely articulated and is exposed laterally (Figure 2). The long neck (at least 14.9 m) is well-preserved with a total of 18 cervical vertebrae. This measurement was estimated based on the maximum centrum length including the anterior condyles with the space for the cartilage assumed. The last cervical articulates with the first dorsal vertebra, and the ventral portion of its centrum is largely eroded. In the original description (Wu et al. 2013), the last cervical vertebra was misidentified as the first dorsal, while the 10th and 11th dorsal vertebrae were misidentified as a single dorsal (the 11th dorsal). Here, we regard the nineteenth vertebra as the first dorsal vertebra based on three reasons. Firstly, the minimum length of the centrum (310 mm) of Cv 19 is less than that of Cv 18 (420 mm) and less than half of that of Cv 17 (730 mm). Secondly, the centrum of Cv 19 bears the typical pleurocoel. Thirdly, the diapophysis of Cv 19 projects more horizontally than that in Cv 18.

Cervical vertebrae

General features

Xinjiangtitan shanshanesis has a total of 18 cervical vertebrae preserved *in situ*. Postaxial cervical centra are opisthocoelous and gradually elongate toward the middle part of the cervical column, and attain their greatest length at Cv 12 (length 1230 mm), then shorten subsequently to become more robust near the cervicodorsal transition (Figure 3). The height of the cervical vertebrae increases posteriorly along the neck, and the last cervical is the highest (about 790 mm). All the cervical centra bear lateral longitudinal pneumatic fossae (LPFs) with well defined edges. The longitudinal pneumatic fossa (LPF) on the axis is single and becomes deeper and anteroposteriorly shorter subsequently. In Cv 3–16, the LPF is divided into anterior and posterior lateral fossae by an oblique ridge, which originates at the middle of the ventrolateral margin of the centrum and projects anterodorsally below the diapophyses. As a contrast, the LPFs are shortened as single triangular fossae with a horizontal dorsal ridge in Cv 1 and Cv 18. All the postaxial cervical centra bear a prominent ventrolateral ridge following the parapophysis. The anterior portion of the ventral surface of the cervical centrum is concave and the posterior portion is flat or slightly convex throughout the postaxial cervical series. A low keel is present on the ventral surface in all postaxial cervical centra. A breakage on Cv 3–5 has damaged the ventral keels, such that only the anterior portion of the keel on Cv 4 and the posterior portion of the keel on Cv 5 are preserved. The ventral keel is present in the mid-posterior portion on the ventral surface of Cv 6. The ventral surfaces of Cv 7–12 are partially damaged and the weekly developed keels are preserved on the mid-posterior portion of the ventral surface. The keel is restricted to the anterior part of the concavity from Cv 13 to the last cervical vertebra. The parapophyses are slightly concave dorsally followed by a prominent ventrolateral ridge on both sides in the postaxial cervical series. The preserved parapophyses are fused with corresponding capitula of cervical ribs. In Cv 13–18, the suture between the parapophysis and the capitulum is well defined. The height to width ratio of the posterior surface of the postaxial cervical vertebrae is greater than 1.1 as in

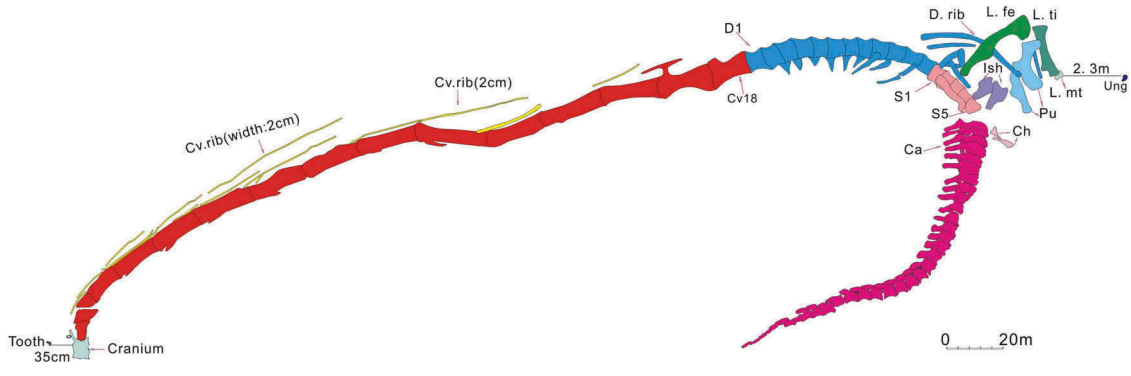

Figure 2. Burial condition of *Xinjiangtitan shanshanesis* (SSV120001).

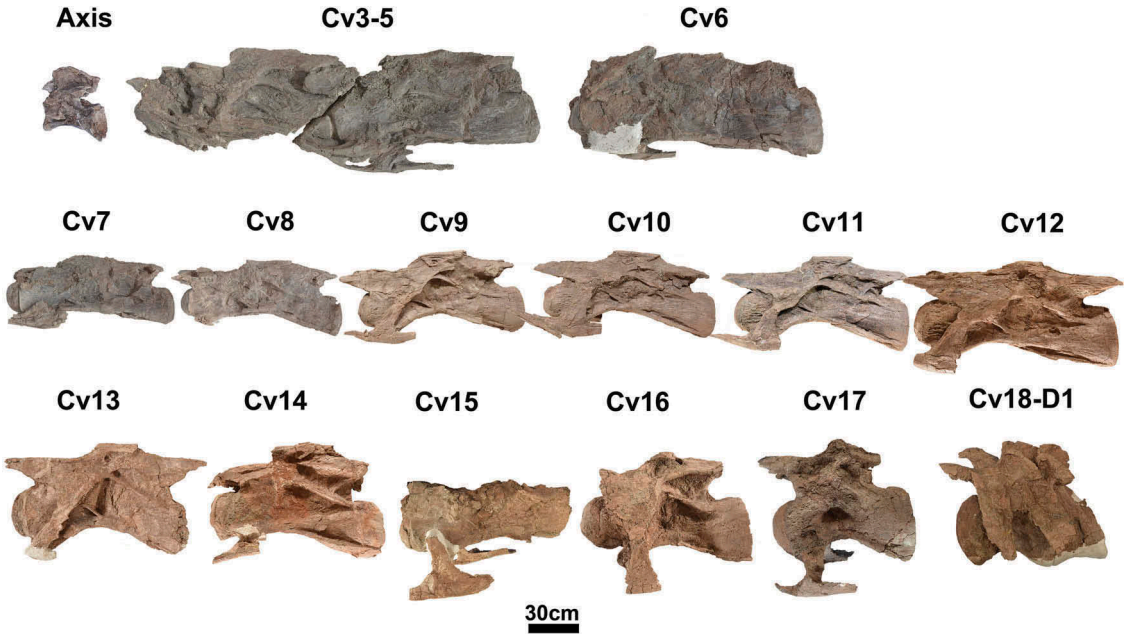

Figure 3. Cv 2-Cv18 of *Xinjiangtitan Shanshanesis* (SSV120001) in left view.

Omeisaurus tianfuensis and *Euhelopus zdanskyi* (He et al. 1988; Wilson and Upchurch 2009)

There are no traces of sutures between the neural arches and centra among cervical vertebrae. The postaxial cervical neural arches are low but increase in height posteriorly along the column. The heights of the neural arch increase dramatically from Cv 13 to Cv 16. The laminae and fossae are well developed on the neural arch. The morphology of the centroprezygapophyseal lamina (CPRL) is single except that in Cv 18, which is dorsally divided and connects the prezygapophysis. All the articular facets of prezygapophyses are weakly convex. The prezygapophyses extend beyond the anterior articular condyle of the centrum; however, the postzygapophyses do not surpass the posterior rim, and from Cv 14 to Cv 18, the postzygapophyses do not reach the posterior limit of the posterior rim. An epipophysis is developed above the postzygapophysis from the axis to Cv 16. A keel is developed in the middle of the spinodiapophyseal fossa (SDF) in Cv 9–11 and Cv 13, which might represent an incipient epipophyseal-prezygapophyseal lamina as in *Mamenchisaurus youngi* (Ouyang and Ye 2002; Wilson et al. 2011). The neural spines are low, anteroposteriorly elongate and horizontal in Cv 3–14, and shortened in Cv 16–17. The neural spines are not bifurcated except that of Cv 18. The neural spine of Cv 18 bifurcates into metapophyses and the median tubercle.

We divide the description into four sections: atlas-axis complex, cervical vertebrae 3–6, cervical vertebrae 7–12 and cervical vertebrae 13–18, based on the features mentioned above, including the locations of the ventral keels, the anteroposterior lengths of the centra and the heights of the cervicals.

Vertebral measurements are provided in Tables 1 and 2. All lengths are anteroposterior, heights are dorsoventral, and widths are transverse widths as seen in anterior or posterior views.

Table 1. Measurements of axis of *Xinjiangtitan shanshanesis* (SSV120001) (in mm).

Centrum	
Length, anteroposterior (including remnant of intercentrum)	195*
Length, anteroposterior	165
Height of posterior articular face	95*
Height of anterior articular face	75*
Breadth of posterior articular face	115*
Breadth of anterior articular face	85*
Minimum breadth,ventral	36*
Neural arch	
Length of postzygapophyses, anteroposterior	62
Breadth of postzygapophyses, mediolateral	55
Length of diapophyses, anteroposterior	60
Breadth of diapophyses, mediolateral	–
Neural canal height, anterior	32*
Neural canal breadth, anterior	40*
Neural canal breadth, posterior	18*
Neural canal height, posterior	35*
Neural spine	
Length of neural spine, anteroposterior	66
Breadth of neural spine, mediolateral	23*
Total height of axis	205

*Indicates a an incomplete or diagenetically distortion measurement.

Atlas-axis complex

Atlas. The atlas is well preserved and includes the atlanteal intercentrum, the odontoid process (atlanteal pleurocentrum), and the neurapophyses (atlanteal arches) (Figure 4). The atlas is preserved *in situ* with the long axis of the intercentrum inclined anterodorsal-posteroventrally, but for convenience of description, we follow directions as in other cervical vertebrae with the intercentrum horizontally oriented.

The intercentrum is crescentic-shaped in both anterior and posterior views. The anterior surface is concave for articulation with the occipital condyle (Figure 4(a)). The dorsal margin of the anterior face is concave and the ventral margin is more anteriorly extended than the dorsal margin. The surface of the dorsolateral edges of the intercentrum is rugose for

Table 2. Cervical vertebral measurements of *Xinjiangtitan Shanshanesis* (SSV120001) (in mm).

Vert	Max Centr Length	Min Centr Length	Pa Width	Max Vert Ht	Di Width	Pleur Foss Ht	Pleur Foss Length	Anter Artc Ht	Anter Artc Width	Poster Artc Ht	Poster Artc Width	Anter Zyg Width	Poster Zyg Width	Neural Arch Ht±	Spin Proc Ht [1]	Spin Proc Ht [2]	SpinProc Max Med-Lat Width[3]	SpinProc Max Anter Poster Length
Ce3	330	260	——	210	45*	70	110	79	70	90	——	55	——	25+	110	——	30	130
Ce4	——	380	60*	260	100^	70	160	80	——	150	——	——	——	——	120	130	30	200
Ce5	——\	565	90*	300	——	125	250	110	——	165	130	——	——	——	140	160	25	220
Ce6	840*	770	100^	330	90*	120	380	160	100	240	160	——	——	——	260	170	20	260
Ce7	1000	890	160^	330	120	140	260	220	150	220	190	——	——	90-	300	175	20	290
Ce8	1090	990	190^	380	——	160	400	200	185	250	200	80	60	80-	330	200	25	330
Ce9	1110	1010	190^	440	130	170	400	220	200	290	220	80	——	100-	330	290	35	330
Ce10	1155	1045	190^	460	220	210	490	270	290	310	375	95	100	110-	350	400	40	370
Ce11	1170	1065	160^	530	——	190	520	320	300	390	260	80	85	110-	380	420	50	300
Ce12	1230	1120	180^	500	220	230	400	390	280	395	295	100	90	110-	430	330	50	200
Ce13	1140*	1025	190^	560	210	270	440	330	295	340	230	100	90	160-	400	460	90	280
Ce14	1150	980	190^	630	——	270	500	340	260	430	360	110	100	140-	300*	430	110	400
Ce15	1050*	990*	160^	——	——	160	390	340	260	——	——	——	——	——	——	——	——	——
Ce16	1140	925	230^	680*	220	260	460	430*	320	510	380	110*	140*	200-*	400	540	85	90
Ce17	850	730	110^	680	——	170	220	400*	380	530	380	155*	160*	210-	280*	510*	90*	110*
Ce18	590	420	60	790	400	270	220	450	390	530*	——	200	90	245+	300	470	190,400	310[#]

Note:*measured distance base on diagenetically distortion; —— distance annot be accurately measured or unsaved; ^measured distance covered by capitulum or tuberculum□Neural Arch Ht+, measured from the ventral magin of neural canal to the ventral magin of prezygapophyses; Neural Arch Ht-, measured from the ventral magin of neural canal to the ventral magin of postzygapophyses; 1, measured from anterioral most point on posteral spinzygapophyseal lamina; 2, measured from dorsal margin of vertebral foramen on the posteral end; and, transverse process(diapophyses fused with the parapophyses)width; 3, if two values given, first, distance between paired metapophyses, second, distance between two triangle lateral precesses; #, the length of bifurcation anteroposteriorly.

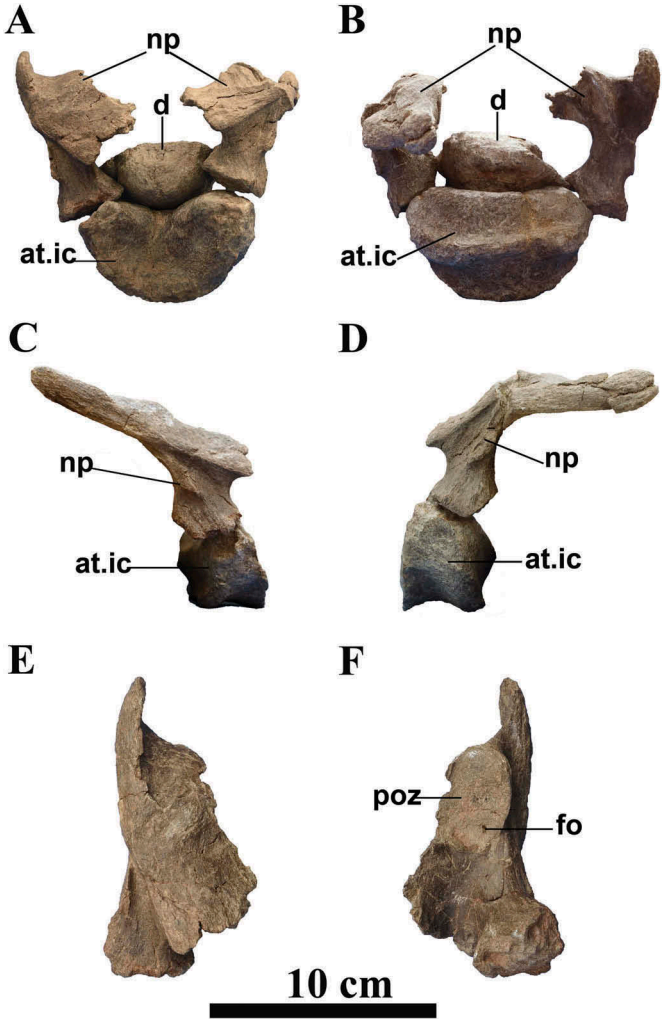

Figure 4. Atlas of the holotype of *Xinjiangtitan shanshanesis* (SSV120001). Atlantal intercentrum, odontoid process and neurapophyses in (a) anterior, (b) posteroventral; (c) right lateral; (d) left lateral views. Neurapophyses in (e) dorsal; (f) ventral views.

articulation with the bases of the neurapophyses on each side, and between them the dorsal face of the intercentrum is slightly concave to receive the odontoid process (Figure 4(a, b)). The posterior face bears an obvious ridge at its mid-height with two small notches on both sides for the atlanteal ribs (Figure 4(b)).

The odontoid process is well preserved. It is short anteroposteriorly (45 mm), wide transversely (70 mm), and approximately trapezoidal in anteroposterior view. Its anterior face is gently concave while the posterior face is convex (Figures 4(a,b); 5(d)). The posterodorsal face of the odontoid is concave to receive the axis (Figures 4(b); 5(b)). The body of the odontoid process tapers slightly posteriorly and bears small lateral processes on both sides.

The neurapophyses (Figure 4) are preserved as long, curved, plate-like elements that approach each other without actually meeting on the midline, and the right neurapophysis is better preserved than the left one. The neurapophysis can be divided into the dorsal and the ventral portions. The dorsal portion is a long, posterodorsally tapering process, while the ventral one bears the large ovoid articular facet for the postzygapophysis (Figure 4(e,f)). A foramen penetrates this facet at its anteromedial corner (Figure 4(f)). The ventral end for articulation with the odontoid is rugose and is almost vertical to the most dorsal end.

Axis. The axis is almost complete but slightly distorted (Figure 6). The anterior articular surface of the axial centrum is flat and circular, with a remnant of the axial intercentrum fused to the ventral portion (Figure 6(a,b,e,f,k,l)). The semicircular and slightly convex articular surface for the odontoid process is just below the neural canal (Figure 6(e,f)). The posterior articular surface is circular and strongly concave. The mid-point of the centrum is transversely compressed and each lateral surface bears a LPF on its lateral surface (Figure 6 (a,b,c,d)). The ventral surface of the centrum is smooth,

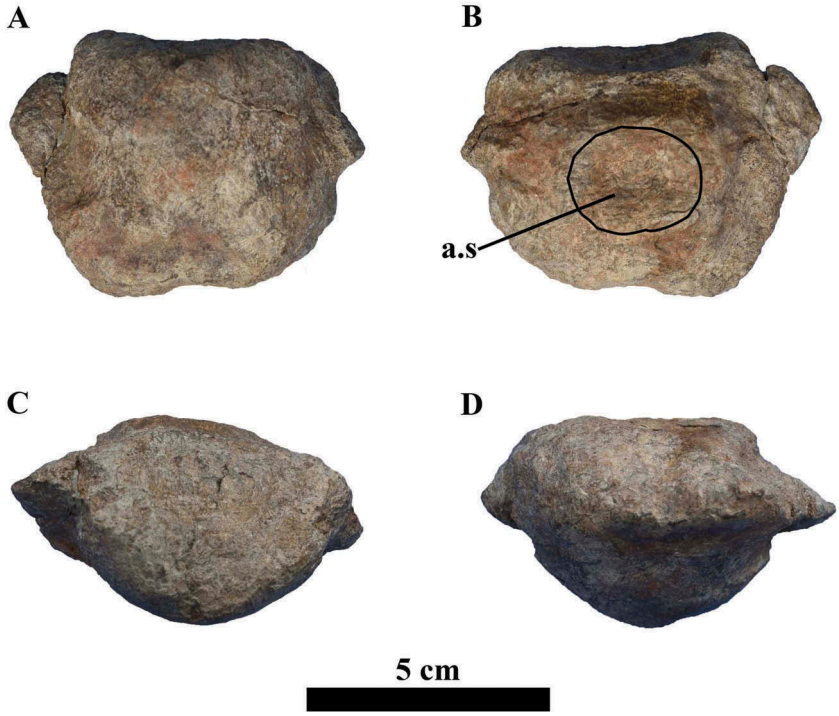

Figure 5. Odontoid process of the holotype of *Xinjiangtitan shanshanesis* (SSV120001). (a) Ventral; (b) posterodorsal; (c) anterior; (d) posterior views.

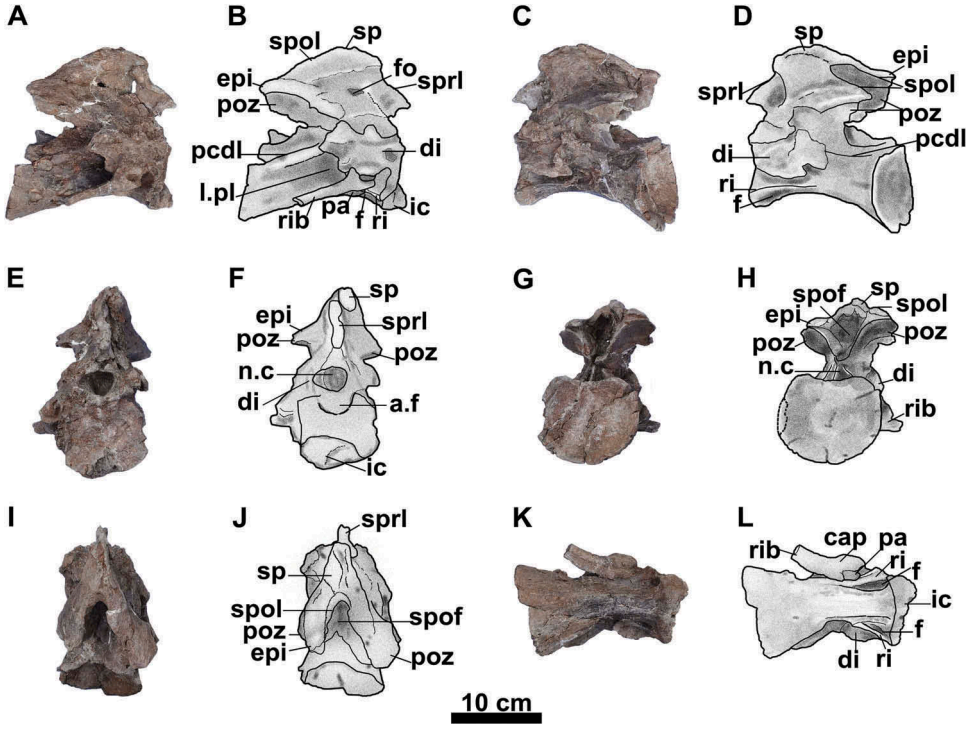

Figure 6. Photographs and interpretive line drawings of the axis of the holotype of *Xinjiangtitan shanshanesis* (SSV120001). (a,b) Right; (c,d) left; (e,f) anterior; (g,h) posterior; (i,j) dorsal; (k,l) ventral views.

slightly convex and lacks a midline ridge. There is a small longitudinal fossa between the ventrolateral ridge and the ventral surface on both sides (Figure 6(a,b,c,d,k,l)).

The right parapophysis is located at the anteroventral corner of the lateral surface of the centrum and articulates with the cervical rib (Figure 6(a,b)). The diapophysis is located at the anterior end of the junction of the neural arch and the centrum. It projects ventrolaterally and connects the rib in right lateral view. The posterior centrodiapophyseal lamina is developed as a round ridge (Figure 6(c,d)).

The neural arch is half the height of the centrum and the two are completely fused. The neural canal is oblong (wider than tall) in anterior view, but taller than wide in posterior view, which was probably caused by distortion (Figure 6(e,f)).

The dorsal margin of the neural spine is longer axially than wide transversely. Only the right spinoprezygapophyseal lamina (SPRL) is partially preserved (Figure 6(e,f,i,j)). The spinopostzygapophyseal laminae (SPOLs) extend from the posterior margin of the neural spine to the postzygapophyses. In posterior view, the SPOLs enclose a large and deep triangular spinopostzygapophyseal fossa (SPOF) (Figure 6(g,h)). In right lateral view, there is a small and deep foramen at the base of the neural spine (Figure 6(a,b)).

Neither prezygapophysis was preserved. The left and right postzygapophyses differ in size due to distortion, with the right one being better preserved. The postzygapophysis does not extend beyond the posterior limit of the centrum. The articular facet of the right postzygapophysis is subcircular, slightly concave and projects ventrolaterally. A prominent epipophysis is present on the postzygapophyses (Figure 6(a, b,c,d,g,h)). In posterior view, the SPOLs enclose a large and deep triangular SPOF (Figure.6(g,h)).

Cervicals 3–6

The cervicals 3–6 are similar in morphology, such as the shallow lateral pleurocoel of the centrum, the low neural arch and neural spine, and the flat dorsal margin of the neural spine.

Cervicals 3–5. The third to fifth cervical vertebrae are articulated with each other, and were slightly deformed by diagenetic compression,evidenced by a crack between Cv 4 and Cv 5. The anterior articular condyle of the third cervical is taller than wide. The length of the anterior condyle is 15% of the minimum centrum length. The posterior surface is oval and concave. Laterally, the LPF is divided by an anterodorsally oblique ridge into a triangular anterior fossa and a quadrilateral posterior one (Figure 7 (a)). The posterior longitudinal pneumatic fossa (P.LPF) dorsally merges into the centrodiapophyseal fossa (CDF) beneath the diapophysis with the latter being deeper. Ventrally, the centra of Cv 3 –5 are poorly preserved. Only a partial broken ventral keel is present on the anterior end of the ventral surface of Cv 4 and a partial keel on the posterior portion of Cv 5 (Figure 7(b)).

The parapophyses of the three vertebrae are situated near the anteroventral margin of the lateral surface. The diapophysis of Cv 4 is well preserved on the left side and forms a triangular process positioned anterodorsal to the neurocentral junction. In lateral view, the posterior centrodiapophyseal laminae (PCDL) extend along the dorsal margin of the centrum and form the dorsal margin of the CDF and LPF in Cv 4 –5 (Figure 7(a,b)).

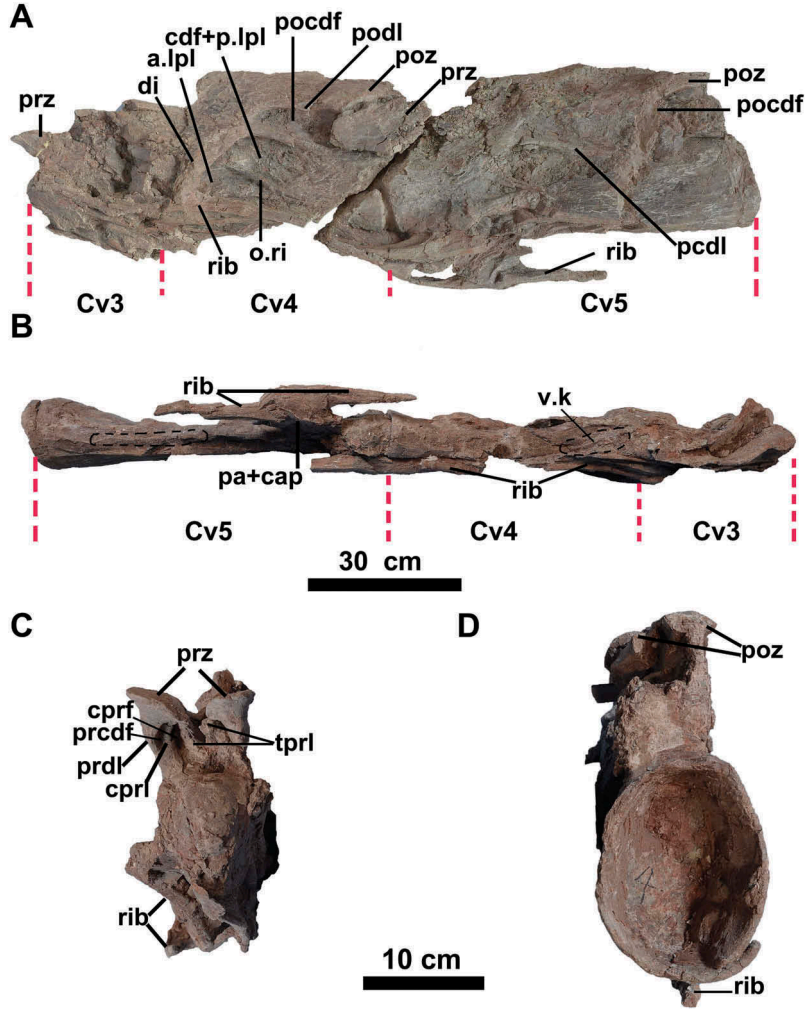

Figure 7. Photographs and interpretive line drawings of the Cv 3–5 of the holotype of *Xinjiangtitan shanshanesis* (SSV120001). (a) Left; (b) ventral; (c) anterior; (d) posterior views.

The prezygapophyses are preserved in Cv 3–5. In anterior view, the prezygapophyseal facets of Cv 3 are longer than wide and slightly convex. The prezygapophyses project dorsomedially and inclines at an angle of approximately 30° to the horizontal (Figure 7(c)). The left and right halves of the intraprezygapophseal laminae (TPRLs) connect each other and form a 'V-shape', which project anteroventrally (Figure 7(c)). The centroprezygapophyseal lamina (CPRL) is a subvertical rod-like structure that braces the right prezygapophysis ventrally, and a deep centroprezygapophyseal fossa (CPRF) is present between the TPRL and the CPRL. The prezygodiapophyseal lamina (PRDL) connects the lateral surface from the right prezygapophysis to the diapophysis, forming the prezygapophyseal centrodiapophyseal fossa (PRCDF) (Figure 7(c)). The postzygapophyseal facets are poorly preserved. In the neural arches of Cv 4 and Cv 5, the postzygodiapophyseal lamina (PODL) is well developed, defining a longitudinal postzygapophyseal centrodiapophyseal fossa (POCDF) (Figure 7(a,b)). The neural spines of the three cervicals are dorsoventrally short and elongate anteroposteriorly (Figure 7(a,b,c)).

Cervical 6. The centrum of Cv 6 becomes more anteroposteriorly elongate than that of Cv 3–5. The anterior articular condyle of the centrum is convex about 11% of the length of centrum (excluding the anterior condyle) (Table 2). The anterior or posterior articular height is greater than the anterior or posterior articular width. Laterally, there is a distinct boundary between the centrum and the anterior articular condyle (Figure 8(a)). A prominent ventrolateral ridge originates from the posterior margin of the parapophysis and extends along the central lateroventral margin. The ventrolateral ridge is flat. The ventral surface of the centrum is sharply concave between the parapophyses but becomes flat posteriorly and bears a ventral keel along the whole ventral surface (Figure 8(c)). The right parapophysis connects the capitulum of the cervical rib that is located at the most anteroventral margin. The right diapophysis is well preserved as a triangular process. It contacts ventrolaterally with the tuberculum of the cervical rib, as in the previous vertebra (Figure 8(a)).

The prezygapophyses and postzygapophyses are not well preserved. The prezygapophyses are compressed and deformed, but the CPRL below the prezygapophysis projects posteroventrally and the SPRL is preserved faintly in right lateral view (Figure 8(a)). The prezygodiapophyseal lamina (PRDL) is compressed, plate-like and overlaps the lateral surface of the centrum and arch. The sheet-like PODL and the ridge-like PCDL outline the POCDF in the right lateral neural arch (Figure 8(a)). The POCDF becomes shallower posteriorly. The CDF is long oblong-shaped. It is present below the diapophysis, and its ventral portion merges with

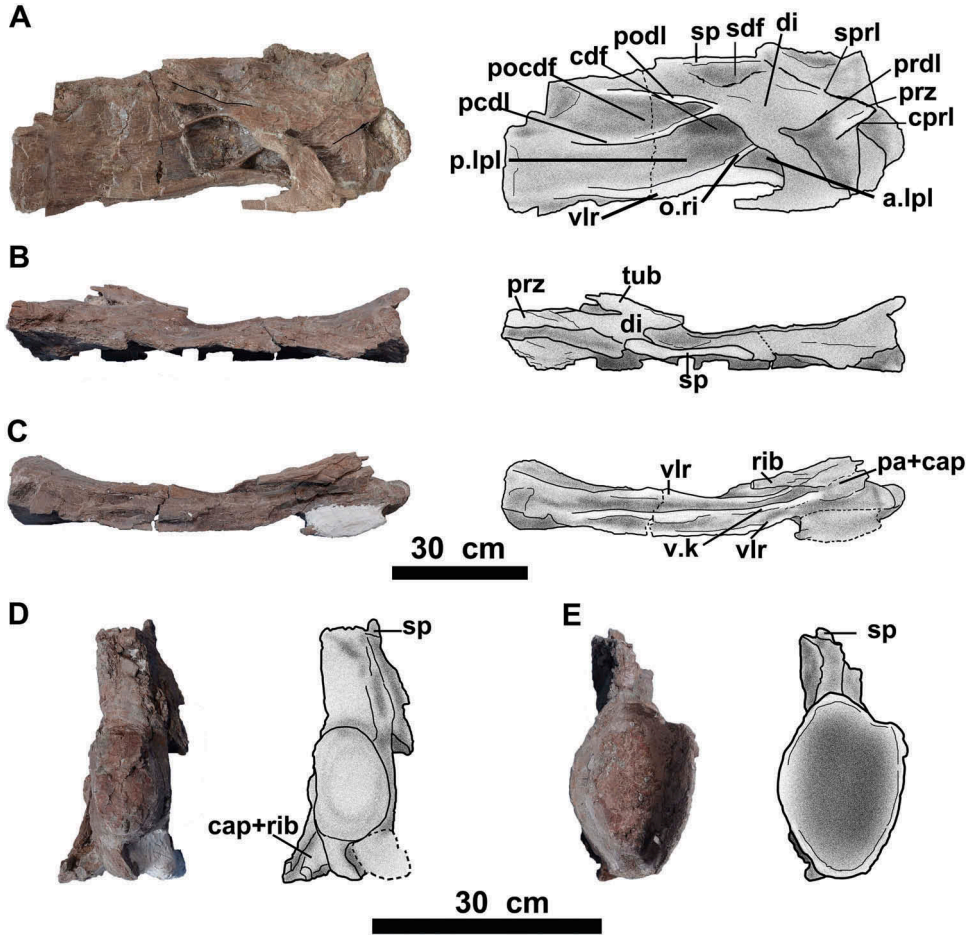

Figure 8. Photographs and interpretive line drawings of the Cv 6 of the holotype of *Xinjiangtitan shanshanesis* (SSV120001). (a) Left; (b) dorsal; (c) ventral; (d) anterior; (e) posterior views.

the central longitudinal pleurocoel (Figure 8(a)). A small and shallow SDF is positioned at the base of the neural spine (Figure 8(a)). The neural spine is narrow transversely, and more elongate anteroposteriorly than that of the previous cervicals (Figure 8(a,b,d,f)).

Cervical 7–12

These six cervical vertebrae are similar morphologically (Figures 3, 9). They are all opisthocoelous, and the anterior condyle comprises 10% of the minimum length of centrum (excluding the anterior condyle length). The central length is about 1 meter in Cv 7 and gradually elongate to 1230 mm at Cv 12, which is the longest cervical in the entire cervical series (Table 2). The lamination and fossae are well developed. In the following description, we will provide a detailed description of Cv 9 as an example of the typical morphologies of the middle cervical vertebrae (Figure 9(a,b,c,d)) is convex. The boundary between the anterior condyle and the lateral surface of the centrum of Cv 9 is also well developed (Figure 9(a)). Both the anterior and posterior articular surfaces are taller than they are wide.Unlike in the previous cervical centra, the ventrolateral ridge of the centrum curves dorsally at its mid-length (Figure 9(a,d)). The LPF is divided by an oblique ridge projecting anterodorsally as in anterior cervical vertebrae (Figure 9(a)). The A.LPF is deeper and the posterior one is shallower than in cervicals 3–6. The CDF deepens and merges with the P.LPF ventrally (Figure 9(a)). Ventrally, the parapophysis and the capitulum of the rib articulate with each other. The ventral surface of the centrum is concave anteriorly with a small breakage and the mid-posterior portion is relatively flat (Figure 9(d)). However, the ventral keel is only seen partially in mid-length on the ventral surface in Cv 9. In Cv 7, Cv 8 and Cv 10, it is preserved partially on the mid-posterior portion of the ventral surface because of erosion.

The heights of the neural arches of the Cv 7–12 are greater than in the anterior cervical vertebrae. Laterally, the PRCDF is present, surrounded by the CPRL, the PRDL and the diapophysis (Figure 9(a)). Conversely, the POCDF is triangular and anteroposteriorly long, and is bounded by the PCDL ventrally, the PODL dorsally and the CPOL posteriorly. In lateral view, there is a posterodorsally inclined ridge in the posterior portion of the POCDF, which is present in Cv 8 –12 but is missing in Cv 7 due to preservation. The fossae were distinctly more complicated in Cv 7–12 than in anterior cervicals.

The prezygapophysis of Cv 9 is an elliptical platform that projects dorsomedially. In anterior view, the CPRL appear as round ridges slanting ventrolaterally underneath the prezygapophyses on both sides, and the PRCDF is present lateral to the CPRL in anterior view as in anterior cervical vertebrae (Figure 9(c)). In lateral view, the prezygapophyses extend beyond the anterior condyle and are supported by the well-developed SPRLs dorsally, the CPRLs ventrally and the PRDLs laterally. The PRDL is deformed by compression, and covers the anterolateral surface of the neural arch and the CPRL. In anterior view, the CPRL is observed on the anterolateral surface of centrum. The postzygapophysis of Cv 9 projects ventromedially with a slightly concave articular facet (Figure 9(b)). The epipophyses sit above the postzygapophyses of Cv 7–11 and extend posteriorly to exceed the postzygapophysis (Figure 9(a,b)), which is similar to the finger-like process lateral to the postzygapophysis in *Qijianglong* (Xing et al. 2015). The postzygapophysis is supported by the CPOL ventrally.

The neural spines are low and almost horizontal except in Cv 9, in which the anterior portion of the neural spine slightly slopes anteroventrally. The transverse width of the neural spine gradually increases from Cv 3 to Cv 12. And the neural spine anteroposterior lengths increase from Cv 3 to Cv 10, but from Cv 11 to further posterior elements, the neural spines shorten slightly. In left lateral view, a small and ovate SDF is located at the base of the neural spine of Cv 9, with a short horizontal keel along the middle (Figure 9(a)). The keel is also present in Cv 10–11, but cannot be recognized in Cv 8 or Cv 12 due to poor preservation. In dorsal view, the neural spine is supported by the SPRL anteriorly and the SPOL posteriorly. The spinoprezygapophyseal fossa (SPRF) and SPOF are present as deep grooves (Figure 9(b)).

Cervicals 13–18

Cv 13–18 are opisthocoelous. The ratio of the length of the anterior condyle to the minimum length of the centrum in Cv 13–18 gradually increases with the anteroposterior lengths of centra shorten, and the ratio is 50% at the last cervical.The neural arches, especially those of Cv 17 and Cv 18, become

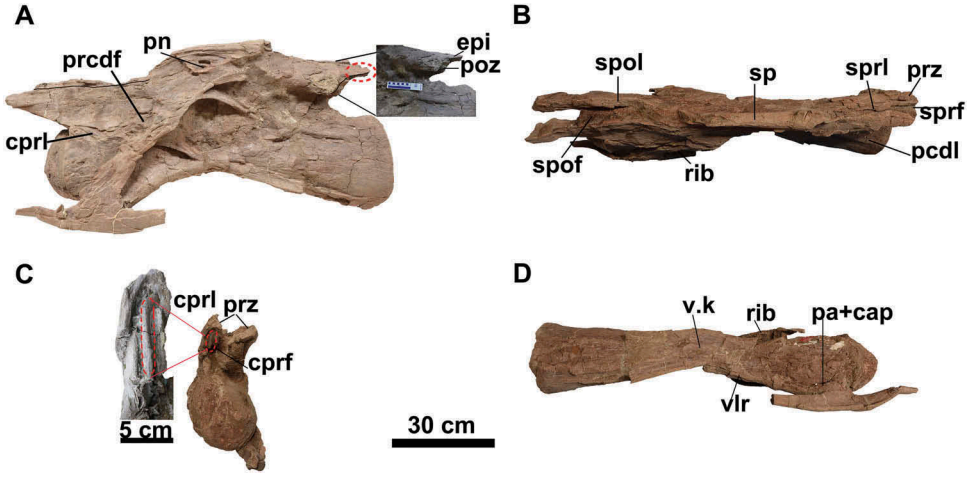

Figure 9. Photographs and interpretive line drawings of the Cv 9 of the holotype of *Xinjiangtitan shanshanesis* (SSV120001). (a) Left; (b) dorsal; (c) anterior; (d) ventral; views.

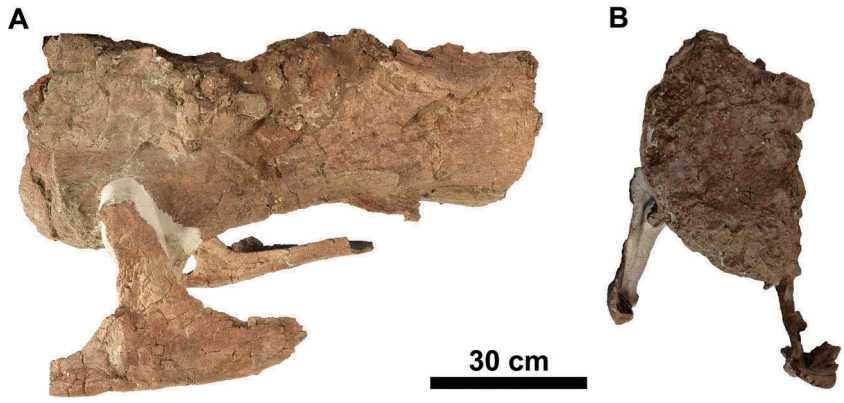

Figure 10. Photographs of the Cervical 15 of the holotype of *Xinjiangtitian shanshanesis* (SSV120001). (a) Left; (b) posterior views.

taller than those in the previous cervical vertebrae. The posterior surface of Cv 13 is damaged; the postzygapophyses and the right parapophysis of Cv 14 are damaged; only the centrum is present in Cv 15; the right parapophysis of Cv 16 is missing; the diapophyses of Cv 17 are absent; and the posteroventral centrum of Cv 18 is missing. The internal pneumaticity is present and can be observed in the centrum of Cv 15 through the damaged surface, like other mamenchisaurids (Figure 10).

Unlike the previous cervical vertebrae, the neural spines of the posterior cervical vertebrae, especially those of Cv 16 and 17, become wider transversely and distinctly shorter anteroposteriorly, and the neural spine bifurcates abruptly in Cv 18.

Cervicals 13–16

The heights of these four cervical vertebrae are greater than all previous cervical vertebrae, although the centra still elongate anteroposteriorly. The centra of Cv13–16 are more strongly constricted at the mid-length than the previous cervical vertebrae are. In Cv 13–16, the ventrolateral ridge of the centrum curves dorsally and becomes thinner (Figure 11(a)) in lateral view. As in previous cervical vertebrae, the LPF of Cv 13–16 (Cv 15 is damaged) is divided by the oblique ridge. In Cv 16, the oblique ridge is thinner and weaker than in the previous cervical series. The A.LPF becomes shallower and smaller while the P.LPF merges with the CDF dorsally. The LPL are obviously deeper and shorter anteroposteriorly than in previous cervicals. Ventrally, the ventral keel is confined to the anterior concavity of the centra except for Cv 15, as a result of a breakage on its ventral surface (Figure 13). The POCDFs become taller as the neural spines progressively increase in height along the column. There is a posteroventral ridge present in posterior portion of the POCDF in Cv 13–14 (Figure 11(a,b,c)).

The parapophyses are gradually more prominent from Cv 13 to Cv 16 (i.e. longer axially and wider transversely) (Figure 11). In left lateral view, the parapophysis of Cv 16 projects more ventrally and bears a distinct suture with the capitulum of rib (Figure 11(c)). The prezygapophysis of Cv 16 is poorly preserved. And the epipophysis is well above the postzygapophysis (Figure 11). The diapophyses of Cv 13-16 are positioned higher on the anterior portion of the neural arch, so that the CDF extends more dorsoventrally and descends to a greater depth than in the previous cervical vertebrae. A short keel is present in the SDF of Cv 13 as in Cv 12, but this feature is absent from Cv 14 to Cv16 (Figure 11). In anterior view, the CPRL slopes posteriorly to connect the dorsal margin of centrum, as in the preceding cervical vertebrae (Figure 12).

The neural spine of Cv 13 is parallel with the anteroposterior axis of the centrum as a longitudinal ridge, and is longer than wide as in previous cervical vertebrae (Figure 11). The anteroposterior length of the neural spine of Cv 14 increases abruptly by distortion (Figures 11(b); 14(b)). The neural spine of Cv 16 shortens anteroposteriorly and its transverse width is almost equal to the anteroposterior length; in addition, the middle portion is higher than both sides, which seems a transitional condition to the bifurcated neural spine (Figures 11(c); 14(c)).

Cervical 17

The centrum of Cv 17 is prominently anteriorly convex with the anterior condyle about 18% of the length of the centrum (excluding the anterior condyle). The length of the centrum decreases by about 25% of that of Cv 16 (Table 2). The anterior part and the posterior part of the centrum have strong transverse expansions, and the middle portion of the centrum constricts distinctly. The LPF observed in previous cervical centra becomes a small and deep subtrianglar fossa (Figure15(a,b)) without the oblique ridge. A horizontal ridge is present dorsally to the lateral pneumatic fossa of the centrum. Unlike the previous cervical vertebrae, the ventrolateral ridge is arched dorsally as a sharp sheet posterior to the parapohysis (Figure 15(a,b)). The parapophysis is wider than long and projects more ventrally than in preceding cervical vertebrae. There is also a clear boundary between the parapophysis and the capitulum of a partial rib (Figure 15(c,e)). Only the base of the diapophysis is preserved and placed higher than in Cv 16. In ventral view, the ventral surface is concave anteromedially and the ventral keel is confined in the concavity (Figure 15(c)). The neural arch is taller and shorter anteroposteriorly than that in Cv 16. The almost vertical CPRL and CPOL support the prezygopophyses and postzygapophyses ventrally respectively. The articular facet of the prezygapophysis of Cv 17 is quadrilateral and projects dorsally (Figure 15(d)). The epipophysis is

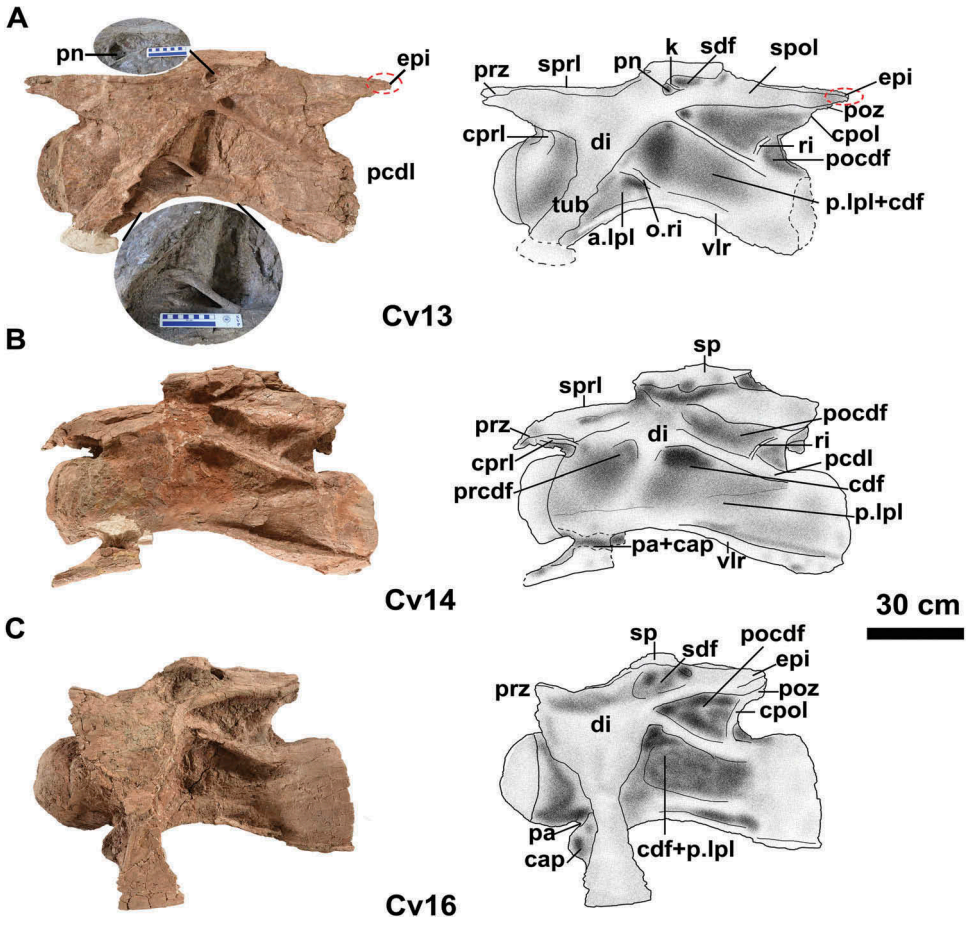

Figure 11. Photographs and interpretive line drawings of the Cv 13, Cv 14 and Cv16 of the holotype of *Xinjiangtitan shanshanesis* (SSV120001) in left view. (a) Cv13 in left; (b) Cv14 in left; (c) Cv16 in left views.

absent, and the articular facet of the right postzygapophysis has a transversely elongate rectangle shape (Figure 15(f)). Laterally, a faint mark of the anterior centrodiapophyseal lamina (ACDL) originates anteroventral to the diapophysis (Figure 15(a)). The ACDL cannot be observed in the preceding cervical vertebrae because it is concealed by the cervical ribs. The PODL is preserved as short sheet-like trace (Figure15 (a,b)).

The neural spine of Cv 17 has a transitional state from the normal to the bifurcated condition. In dorsal view, the neural spine splits into a slightly concave middle portion and expanded two sides. The SPRL, the SPRF, the SPOL and the SPOF are developed (Figure 15(d)). In lateral view, the SDF is present as a small and deep fossa at the base of the neural spine without the keel observed in previous cervicals (Figure 15(a,b,c)).

Cervical 18

The eighteenth vertebra is preserved articulated with the nineteenth vertebra. The posteroventral portion of the centrum and the mid-ventral portion of the nineteenth centrum are missing. We take the eighteenth vertebra as the Cv18 (last cervical) and the nineteenth vertebra as the first dorsal vertebra as aforementioned.

Cv 18 is the anteroposteriorly shortest cervival vertebra (Table 2). It is strongly opisthocoelous, and the anterior condyle protrudes anteriorly about a half of the minimum length of centrum excluding the anterior condyle. There is also a clear boundary between the anterior articular condyle and the lateral surface of the centrum. In lateral view, the anterior and posterior portions of the centrum expand more strongly and the middle part of the centrum constricts more distinctly than in Cv 17. A horizontal ridge is present dorsal to the LPF as in Cv 17 (Figures 15, 16, 18). The ventrolateral ridge is present as a short, arcuate ridge. The ventral surface of the centrum in Cv 18 is pinched transversely with no ventral ridge.

The neural arch is considerably taller than that in preceding cervicals and the laminae are well developed. In right lateral view, the base of the diapophysis is situated on the anterodorsal portion of neural arch. The triangular CDF is surrounded by the PCDL and the ACDL, as in Cv17. ThePRDL, the ACDL, and the CPRL enclose an oblique oval PRCDF with some deformation in right lateral view (Figure 16(b)).

Contrasting with previous cervicals, the remarkable feature of Cv 18 is the bifurcation of the neural spine. The neural spine bifurcates into two hemispinous processes (one half of a bifurcate spinous process = metapophysis *sensu*, Harris 2006) setting off from a median tuberculum (Hatcher 1901; Wiman 1929; Gilmore 1936; Harris 2006) by intraspinous sulci. The metapophyses

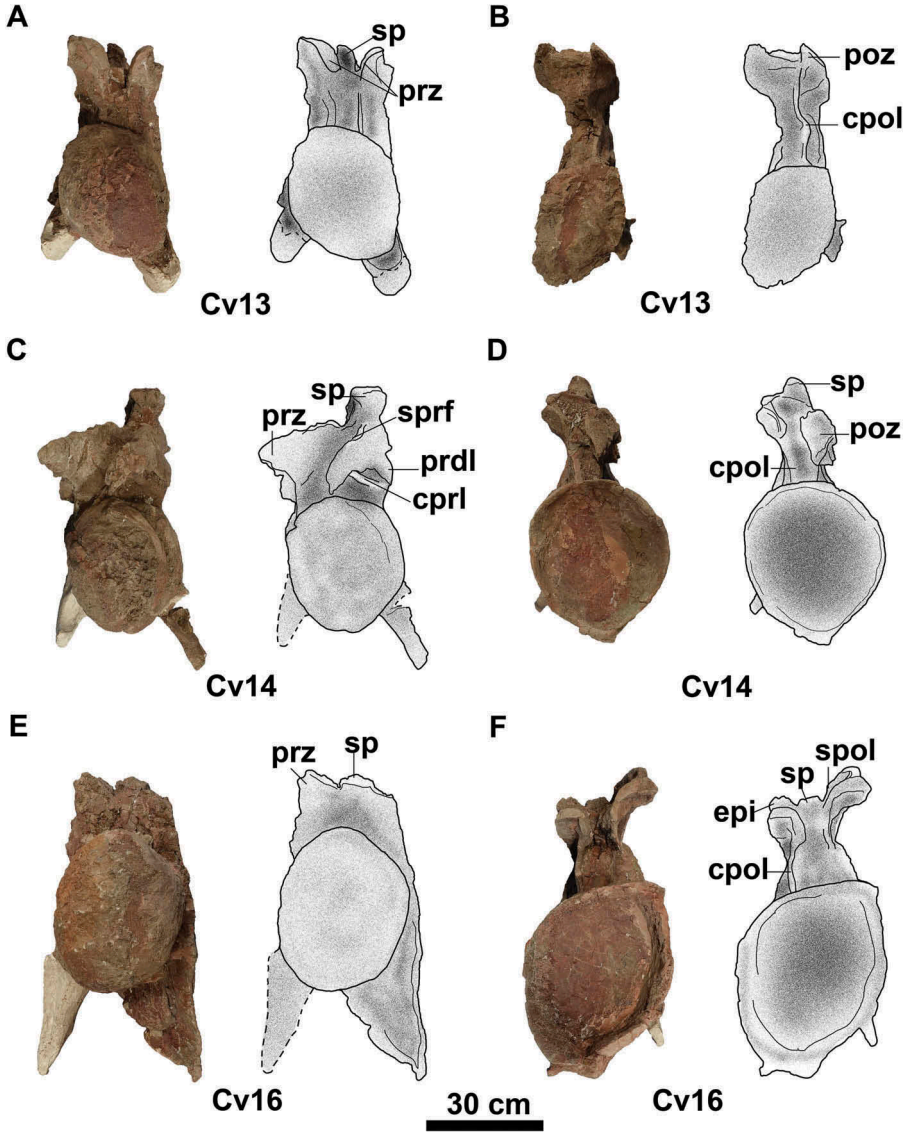

Figure 12. Photographs and interpretive line drawings of the Cv13, Cv14 and Cv16 of the holotype of *Xinjiangtitian shanshanesis* (SSV120001) in anterior and posterior views. (A) Cv13 in anterior; (b) Cv13 in posterior; (c) Cv14 in anterior; (d) Cv14 in posterior; (e) Cv16 in anterior; (f) Cv16 in posterior views.

extend posterolaterally as a triangular lateral process covering the SPOL. The bifurcation area forms a 'W'-shape in dorsal view, and forms a 'U'-shape in posterior view. (Figures 16, 17, 18). The SDF is divided into upper and lower fossae by a horizontal ridge as on Cv 8–13, whereas the upper one of Cv 18 is further divided by an anterodorsal ridge from the posterior part of the horizontal ridge to middle part of the SPRL (Figures 16(a), 17(b)).

The parapophysis projects laterally with an oval articular facet (Figure 16(a,b)). The left diapophysis is oriented laterally (Figures 16(a), 17(b)). The right diapophysis is poorly preserved and raised by deformation. The prezygapophysis is located more dorsally than in Cv 17, and the right prezygapophysis is larger than the left one because of distortion. The articular facet of the prezygapophysis is slightly convex and quadrilateral. In anterior view, the CPRL dorsally splits into two ridges close to the ventral surface of the prezygaophysis. Both TPRLs connect with each other as a 'V'-shape between the prezygapophyses. The PRCDF and the CPRF are separated by the CPRL. The postzygapophyses of Cv 18 cannot be described because it is articulated with dorsal vertebra 1. (Figures 16, 17, 18).

Cervical ribs

All cervical ribs except those on Cv 8, Cv 11, Cv 15 and Cv 18 are preserved in fragments and their proximal articular surfaces articulated with the centra. As in other sauropod dinosaurs, cervical ribs are tetraradiate and double-headed comprising a short anterior process, a capitulum, a tuberculum, and a long, slender, posteriorly-directed main shaft with developed medial groove, which is different from that in *Shunosaurus lii* (Zhang 1988). The anterior process of cervical rib is short, dagger-like with pointed-end as in *Mamenchisaurus hochuanensis* (Yang and Zhao 1972). The tuberculum is plate-like and it is proximally fused with the diapophysis without sutures in Cv 3 -Cv 16 except for in Cv 8, Cv 11, Cv 15 and Cv 18, in which the tuberculum is not preserved. The capitulums are column-like and shorter than

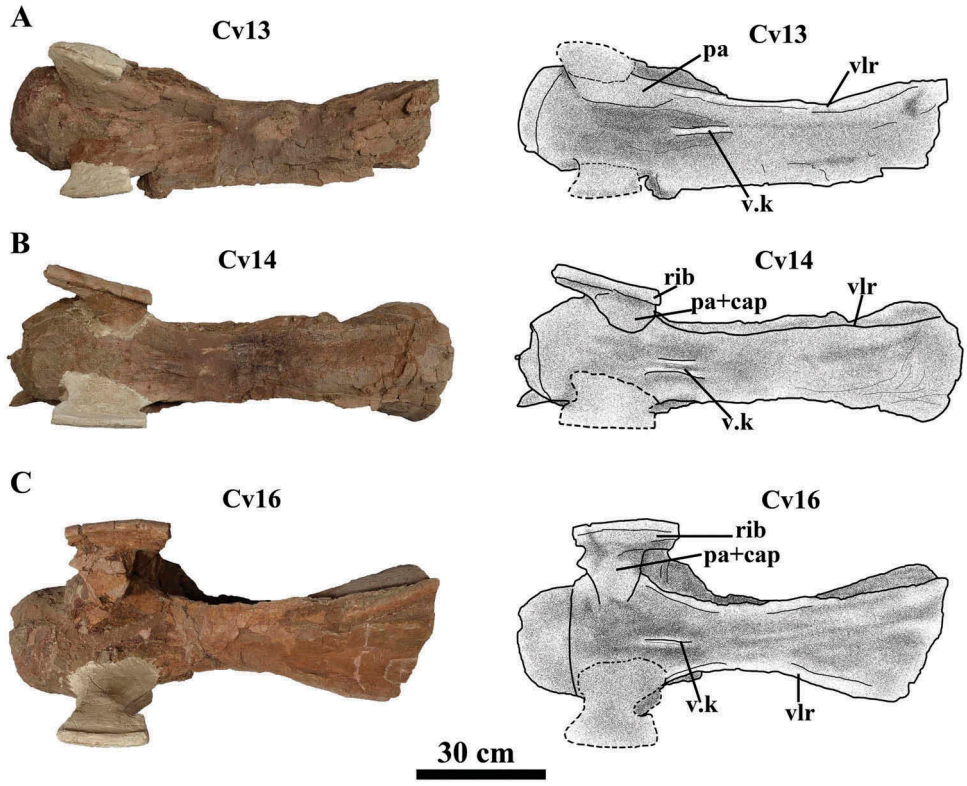

Figure 13. Photographs and interpretive line drawings of the Cv13, Cv14 and Cv16 of the holotype of *Xinjiangtitian shanshanesis* (SSV120001) in ventral view. (a) Cv13 photographs and interpretive line drawings; (b) Cv14 photographs and interpretive line drawings; (c) Cv16 of photographs and interpretive line drawings.

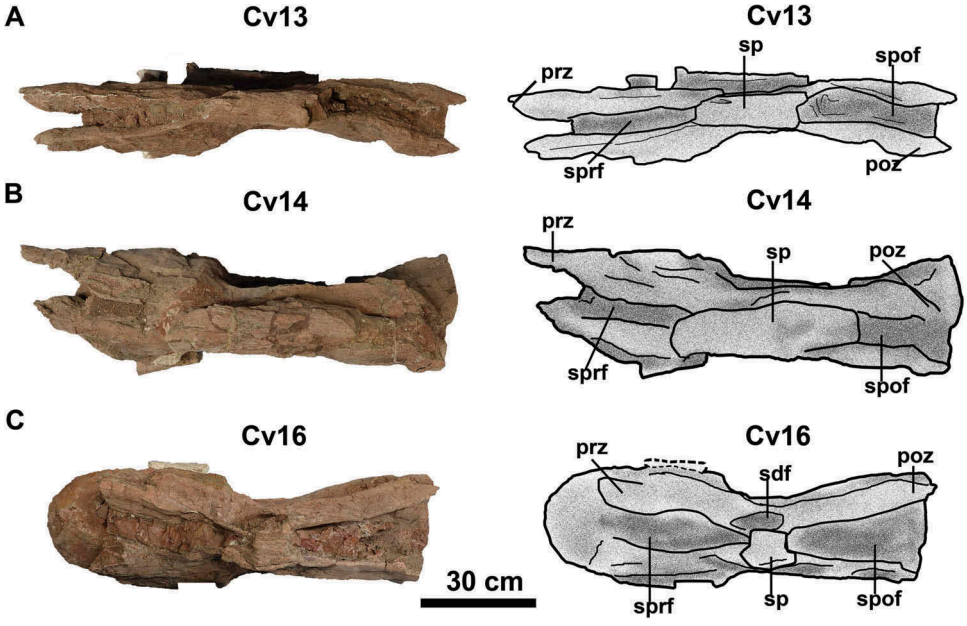

Figure 14. Photographs and interpretive line drawings of the Cv13, Cv14 and Cv16 of the holotype of *Xinjiangtitian shanshanesis* (SSV120001) in dorsal view. (a) Cv13 photographs and interpretive line drawings; (b) Cv14 photographs and interpretive line drawings; (c) Cv16 of photographs and interpretive line drawings.

the tuberculum, which fused/semi-fused to the parapophyses. However, from Cv 15 to Cv 18, the degree of the fusion of cervical ribs gradually decreases and distinct sutures between the capitulum and parapophysis are present (Figures 11(c), 15).

Some isolated partial cervical ribs were found *in situ* (Figure 2). One cervical rib, with a diameter of about 200 mm, elongate anteroposteriorly to extend to the next three cervical vertebrae or the anteriority of the next four cervical (Figure 2) as in *Mamenchisaurus hochuanensis* (Yang and Zhao 1972), but differ from *Euhelopus* (Wilson and Upchurch 2009), in which the rib only extends to the next cervical. This may indicate that *Xinjiangtitan shanshanesis* has a long thick neck. Another isolated right rib is preserved

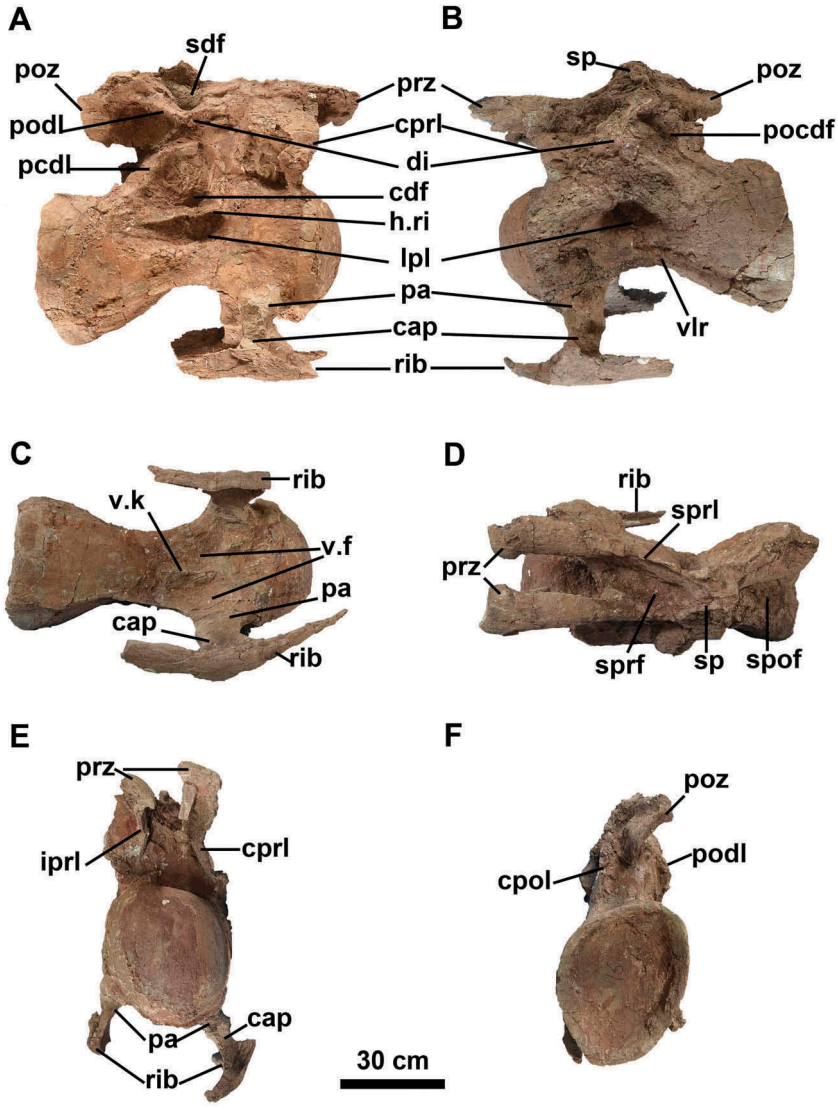

Figure 15. Photographs and interpretive line drawings of the Cv 17 of the holotype of *Xinjiangtitan Shanshanesis* (SSV120001). (a) Right lateral; (b) left lateral; (c) ventral; (d) dorsal; (e), anterior; (f) posterior views.

with the capitulum and a partial posterior shaft. The capitulum is a dorsoventrally elongated column-like process. In anterior view, the proximal portion curves laterally slightly. The preserved posterior potion of the shaft is medially concave with the base of the tuberculum, and the shaft tapers posteriorly to become a slender rod. The middle portion of the shaft is convex laterally (Figure 19).

Comparison and discussion

Wu et al. (2013) proposed that the cervical vertebrae of *Xinjiangtitan shanshanesis* bore two diagnostic features: the first is that a keel developed on the one fourth of the ventral surface of the penultimate cervical centrum and formed a small semi-circular process under the posterior articular facet; the second is that the last two cervical centra are particularly elongated (ratio 'total length of the last two cervical vertebrae: total length of femur and tibia' is 0.63). Our redescription has shown that neither of these two features is accurate.

Firstly, the penultimate cervical identified by Wu et al. (2013) is actually the antepenult cervical (Cv 16), and the small semi-circular process under the distal articular surface is not a natural morphology, while it is actually a deformed portion of the posterior articular surface of the centrum caused by diagenetic compression (Figure 12(f)). Secondly, the total number of the cervical vertebrae is 18, and the last cervical vertebra (Cv 18) was mistaken for the first dorsal vertebra by Wu et al. (2013). Finally, the last two cervical vertebrae are shorter than the preceding cervicals, and the ratio 'length of the last two cervical vertebrae: length of femur and tibia' is 0.34, not 0.63 as reported by Wu et al. (2013). This value is 0.31 in *Mamenchisaurus youngi*, Ouyang and Ye (2002), and given incompleteness of other mamenchisaurid specimens, no meaningful comparison can be made based on such a value.

In light of the research conducted by Wu et al. (2013), comparisons will be made here limited to some mamenchisaurid dinosaurs with relevant skeletal parts preserved.

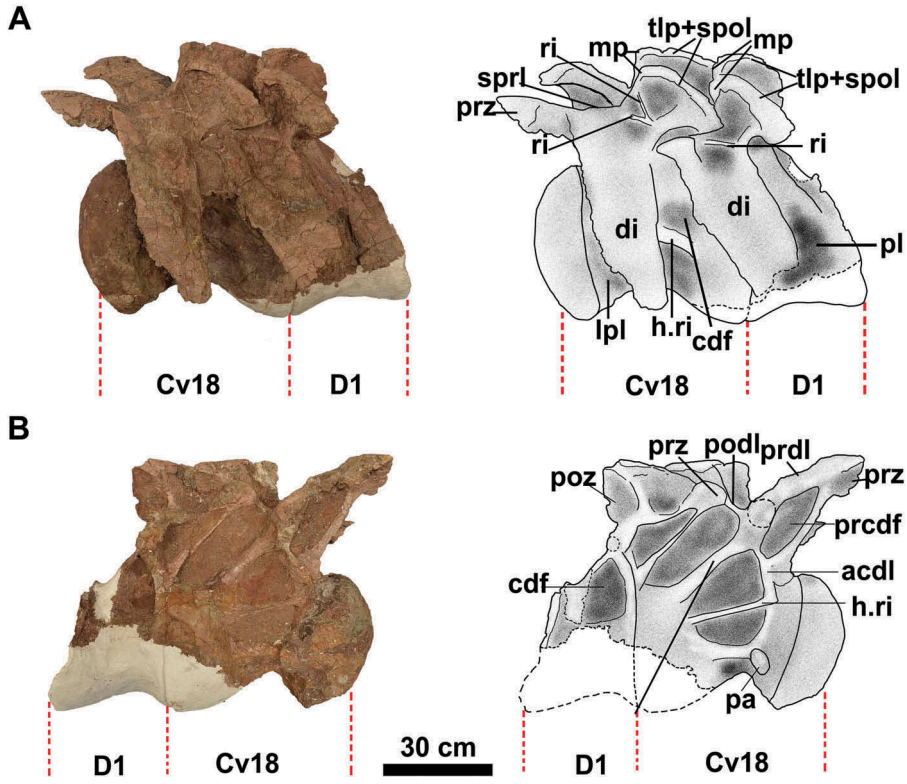

Figure 16. Photographs and interpretive line drawings of the Cervical 18 and Dorsal 1 of the holotype of *Xinjiangtitan shanshan*esis (SSV120001) in lateral views. (a) Left lateral; (b) right lateral.

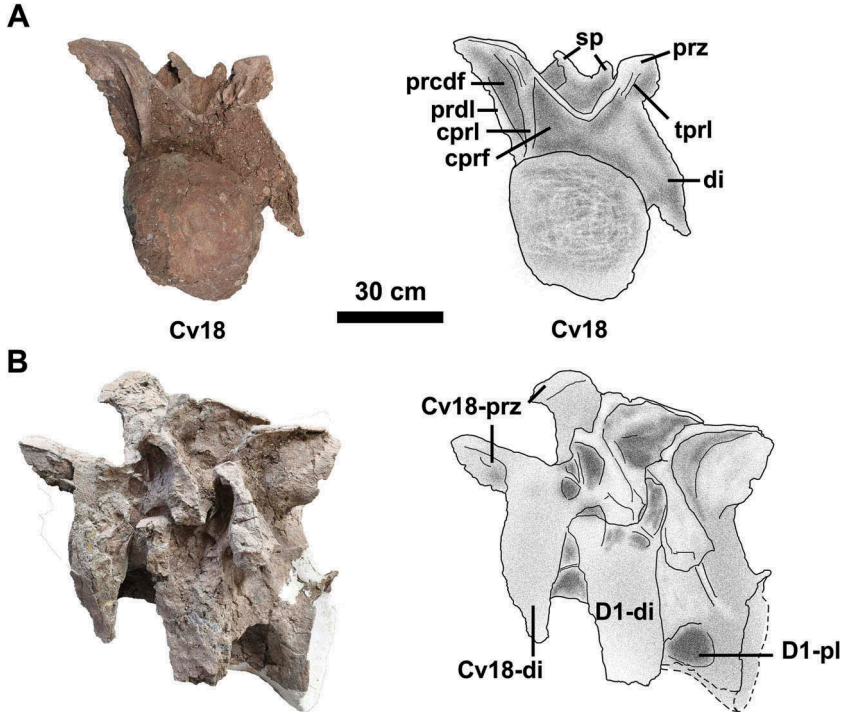

Figure 17. Photographs and interpretive line drawings of the Cervical 18 and Dorsal 1 of the holotype of *Xinjiangtitan shanshan*esis (SSV120001) in anterior and left posterior views. (a) Anterior; (b) left posterior views.

Mamenchisaurus sinocanadorum

Mamenchisaurus sinocanadorum (Russell and Zheng 1993) was discovered from the Shishugou Formation of the Late Jurassic in the eastern Junggar Basin of Xinjiang. Features shared between *Mamenchisaurus sinocanadorum* and *Xinjiangtitan shanshanesis* include prominent longitudinal ventrolateral ridges on the axis

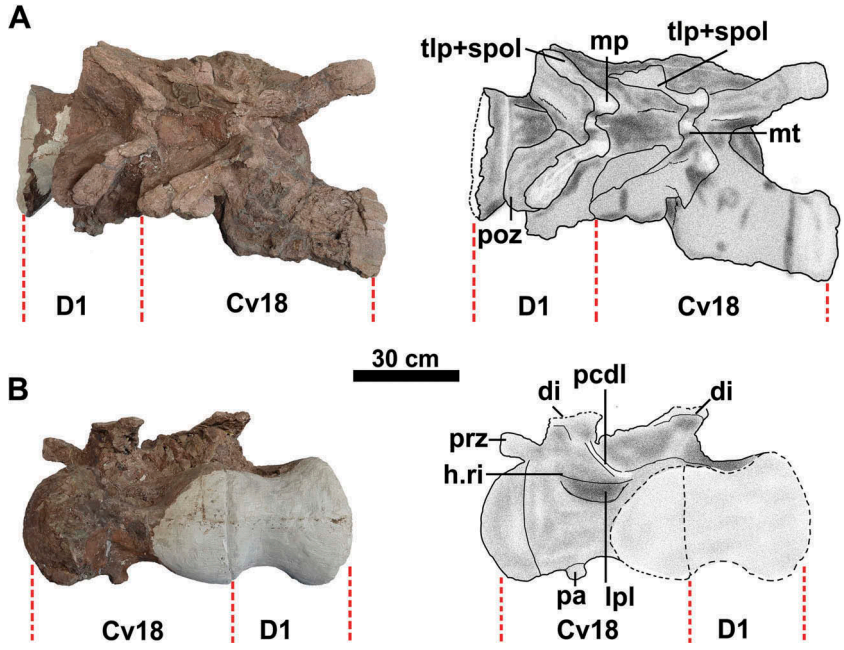

Figure 18. Photographs and interpretive line drawings of the Cervical 18 and Dorsal 1 of the holotype of *Xinjiangtitan shansha*nesis (SSV120001) in dorsal and ventral views. (a) Dorsal; (b) ventral views.

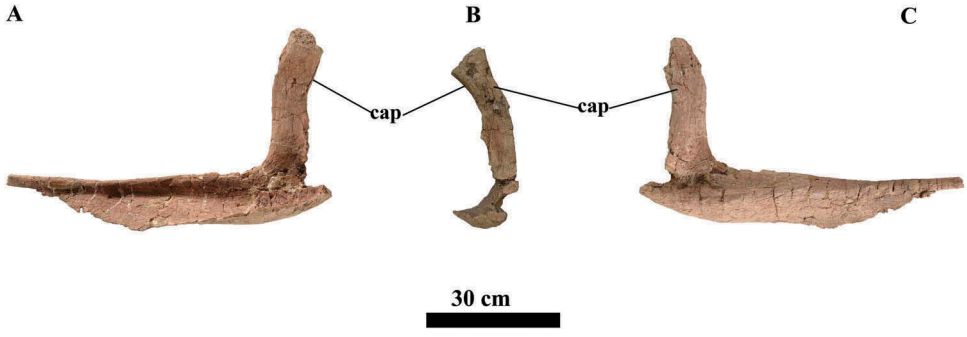

Figure 19. Partial right cervical rib of *Xinjiangtitan shanshanesis* (SSV120001). (a) Right; (b) anterior; (c) left views.

and successive cervical centra. Differences between these taxa are that the axial neural spine in *Xinjiangtitan shanshanesis* is higher than the crest of the zygapophyseal rami (whereas the neural spines of the axis and Cv 3 lie below the crest of zygapophyseal rami in *Mamenchisaurus sinocanadorum*); the axial epipophysis of *Xinjiangtitan shanshanesis* is a small process (whereas it is well developed in *Mamenchisaurus sinocanadorum*); the axis and subsequent cervical centra of *Xinjiangtitan shanshanesis* lack small foramina beneath the diapophysis (whereas small foramina are present beneath the diapophysis in *Mamenchisaurus sinocanadorum*); the axis of *Xinjiangtitan shanshanesis* lacks a visible suture between the neural arch and the centrum (whereas the suture is observable in *Mamenchisaurus sinocanadorum*); the cervical lateral pneumatic fossae are complex and divided by an bony ridge in all postaxial cervicals of *Xinjiangtitan shanshanesis* (whereas the cervical lateral pneumatic fossae are simple and undivided in the anterior cervicals of *Mamenchisaurus sinocanadorum*); and the length of the fourth cervical centrum is 1.46 times that of the third cervical centrum in *Xinjiangtitan shanshanesis* (whereas this ratio in *Mamenchisaurus sinocanadorum* is 1.27).

Mamenchisaurus constructus

Mamenchisaurus constructus was first discovered in 1952 from the Jurassic beds on the construction site of Yitang Highway in Sichuan. The partial skeleton fossil was named as *Mamenchisaurus constructus* by Young in 1954.

The neck of *Mamenchisaurus constructus* preserves 14 cervical vertebrae, but few of these are preserved in a good condition (Young 1954, 1958). The total length of the cervical column of *Mamenchisaurus constructus* (4670 mm) (Young 1954, 1958) is one third of the total length of the cervical column of *Xinjiangtitan shanshanesis*. The ventral surfaces of the cervical centra of *Xinjiangtitan shanshanesis* have prominent keels, whereas in *Mamenchisaurus constructus* the centra are concave ventrally and lack the ventral keels.

Mamenchisaurus hochuanensis

Mamenchisaurus hochuanensis was discovered from the Upper Shaximiao Formation in the Sichuan Basin (Yang and Zhao 1972). *Xinjiangtitan shanshanesis* differs from

Mamenchisaurus hochuanensis (Yang and Zhao 1972) in that the number of cervical vertebrae is 18 (vs. 19 in *Mamenchisaurus hochuanensis*); the cervical lateral pneumatic fossae are well developed and divided by bony septa in all post-axial cervicals (vs. poorly developed and relatively simple cervical lateral pneumatic fossae in the post-axial cervicals of *Mamenchisaurus hochuanensis*); the ratio of the length of Cv 3 to Cv2 is 1.58 (vs. 1.34 in *Mamenchisaurus hochuanensis*); and only the last cervical neural spine bifurcates in *Xinjiangtitan shanshanesis* with a median tubercle (whereas all cervical neural spines are bifurcated in the *Mamenchisaurus hochuanensis*, Yang and Zhao 1972: P3).

Mamenchisaurus anyuensis

Mamenchisaurus anyuensis (He et al. 1996) was found from both the Upper Jurassic Penglaizhen Formation and the top of the Upper Jurassic Suining Formation. Specimens of *Mamenchisaurus anyuensis* were estimated to include ten individuals (He et al. 1996). Specimen AL001 includes eight middle to posterior cervical vertebrae. Unlike *Xinjiangtitan shanshanesis*, the centra of *Mamenchisaurus anyuensis* have poorly developed pneumatic fossae (He et al. 1996). Some of the most posterior cervical neural spines are extremely weakly bifid in *Mamenchisaurus anyuensis* (whereas only the last cervical neural spine is bifurcated with a median tubercle in *Xinjiangtitan shanshanesis*). Lastly, in *Mamenchisaurus anyuensis* only the posterior cervical vertebrae have well-developed laminae and fossae, whereas they are developed through the whole cervical series in *Xinjiangtitan shanshanesis*.

Mamenchisaurus youngi

Mamenchisaurus youngi was unearthed from the Upper Shaximiao Formation in Xinmin County, Zigong City in Sichuan Province, China, in 1989 (Ouyang and Ye 2002) and it includes an articulated cervical series. *Xinjiangtitan shanshanesis* shares the following similarities with *Mamenchisaurus youngi* (Ouyang and Ye 2002): the number of cervical vertebrae in both taxa is 18; the occipital facet of atlanteal intercentrum is rectangular in lateral view; the axis does not bear well-developed epipophyses above the postzygapophyses; the ratio of the anteroposterior central length to the dorsoventral height of the posterior articular cotyle of the middle cervical vertebrae is less than 4.0 (the ratio is 3 in Cv 11 in *Xinjiangtitan shanshanesis* and 2.7 in Cv 11 in *Mamenchisaurus youngi*). In *Xinjiangtitan shanshanesis*, a subtle horizontal keel subdivides the spinodiapophyseal fossa in Cv 9–13 and Cv 18 (Figures 9(a), 11(a)), and similar keels are present in some middle cervicals of *Mamenchisaurus youngi* (Ouyang and Ye 2002: Figure 15 (e), H; Wilson et al. 2011), which were interpreted as incipient epipophyseal-prezygapophyseal laminae by Wilson et al. (2011). Despite these similarities, there are still several differences between the two taxa: in *Xinjiangtitan shanshanesis*, the ventral surface of the axis bears a longitudinal fossa on both sides without ridges (whereas in *Mamenchisaurus youngi* there is no fossa, but with low round ridge, Ouyang and Ye 2002); the posterior surface of centrum is circular and strongly concave (whereas the posterior surface is slightly concave in *Mamenchisaurus youngi*, Ouyang and Ye 2002: tab.8); the cervical lateral pneumatic fossae are divided by bony septa in all post-axial cervical vertebrae (whereas the fossae are undivided in anterior cervicals and divided by bony septa in middle-posterior cervicals in *Mamenchisaurus youngi*); the ratio of the length of Cv 3 to Cv 2 is 1.58 (vs. 1.37 in *Mamenchisaurus youngi*); a horizontal ridge is present dorsal to the lateral pleurocoel of the last two cervical centra (vs. lack of the horizontal ridge in *Mamenchisaurus youngi*); the last cervical neural spine is bifurcated with a median tubercle (vs. the bifurcation of cervical vertebral neural spines present in last two cervicals of *Mamenchisaurus youngi*).

Mamenchisaurus jingyanensis

Mamenchisaurus jingyanensis (Zhang et al. 1998) is from the Late Jurassic Upper Shaximiao Formation of the Sichuan Basin. The paratype includes three cervical vertebrae, but only Cv 5 is completely preserved. Cv 5 of *Mamenchisaurus jingyanensis* bears well-developed lateral pneumatic fossae as in *Xinjiangtitan shanshanesis*, but lacks ventral keels, distinguishing *Mamenchisaurus jingyanensis* from *Xinjiangtitan shanshanesis*. The complex laminae and fossa are present in the whole cervical series in *Xinjiangtitan shanshanesis*, whereas the materials of *Mamenchisaurus jingyanensis* are poorly preserved and the description in the original paper is too simple for further comparations

Omeisaurus tianfuensis

Omeisaurus tianfuensis (He et al. 1988) was discovered in the Lower Shaximiao Formation of the Sichuan Basin. The holotype of *Omeisaurus tianfuensis* (He et al. 1988) was estimated to have 17 cervicals (He et al. 1988). As in *Omeisaurus tianfuensis* (He et al. 1988), the postaxial cervical centra of *Xinjiangtitan shanshanesis* bear median keels in the ventral concavities. However, the ventral surface of the axial centrum in *Xinjiangtitan shanshanesis* bears no median ridge (vs. acute ventral median ridge in the axis of *Omeisaurus tianfuensis*); the lateral pneumatic fossa of *Xinjiangtitan shanshanesis* is divided by an anterodorsally oblique ridge into a triangular anterior fossa and a quadrilateral posterior fossa (vs. the lateral pneumatic fossa being divided into several small fossae by1-3 ridges in *Omeisaurus tianfuensis*); the last cervical neural spine bifurcates in *Xinjiangtitan shanshanesis* (vs. no bifurcation in the posterior cervical neural spines of *Omeisaurus tianfuensis*); the lamination is well developed in all postaxial cervicals in *Xinjiangtitan shanshanesis* (vs. lamination only being developed in the last two cervical vertebrae in *Omeisaurus tianfuensis*).

Omeisaurus maoianus

Omeisaurus maoianus (Tang et al. 2001) was from the Upper Shaximiao Formation in Jinyan, Sichuan. Only three cervical vertebrae are preserved in the holotype of *Omeisaurus maoianus* . It differs from *Xinjiangtitan shanshanesis* as a keel is present in the anterior concavity of the ventral surface in Cv 11, and the anterior end of the prezygapophysis does not extend beyond the anterior condyle of the centrum (vs. the

prezygapophysis extending anteriorly beyond the anterior condyle of the centrum in *Xinjiangtitan shanshanesis*).

Qijianglong guokr

Qijianglong guokr was discovered in the Upper Jurassic Suining Formation in the Sichuan Basin (Xing et al. 2015). In *Xinjiangtitan shanshanesis*, pneumatopores are present in the SDFs in the middle-posterior cervical vertebrae, whereas they are also present in the posterior cervical vertebrae in *Qijianglong guokr* (Xing et al. 2015). A subtle keel subdivides the SDF in the middle-posterior cervical vertebrae of *Xinjiangtitan shanshanesis*, and a similar feature is also present in Cv 16 and Cv 17 of *Qijianglong guokr* (Xing et al. 2015: Figure 12(e,f)). In *Xinjiangtitan shanshanesis*, the epipophysis with a tapering end is present on the postzygapophysis and extends posteriorly to exceed the postzygapophysis distinctly in Cv7-14 (Figures 9, 10). The feature is similar to *Qijianglong guokr*, in which a finger-like process is above the postzygapophysis and posteriorly exceed the postzygapophysis distinctly in Cv 5–14 (Xing et al. 2015: Figures 11, 12). Differences between the two taxa include that the number of cervical vertebrae is 18 in *Xinjiangtitan shanshanesis* (vs. 17 in *Qijianglong guokr*); the anterodorsal surface of the atlanteal intercentrum of *Xinjiangtitan shanshanesis* is deeply concave (vs. slightly concave in *Qijianglong guokr*, Xing et al. 2015); the posterodorsal face of the atlas slopes posteriorly to form a prominent ridge in *Xinjiangtitan shanshanesis* (whereas this ridge is absent in *Qijianglong guokr*).

Chuanjiesaurus anaensis

Chuanjiesaurus anaensis (Fang et al. 2000) was discovered from the Chuanjie Formation (Middle Jurassic of Lufeng). The referred specimen of *Chuanjiesaurus anaensis* possesses 11 (axis to twelfth) articulated cervical vertebrae (Fang et al. 2000; Sekiya 2011). *Chuanjiesaurus anaensis* differs from *Xinjiangtitan shanshanesis* in the following features: the axial neural spine of *Chuanjiesaurus* is lower and more elongate anteroposteriorly than that in *Xinjiangtitan shanshanesis* (Sekiya 2011: Figure 6); the ventral surfaces of the postaxial cervical centra are almost flat and lack the ventral midline keels in *Chuanjiesaurus anaensis*. In *Xinjiangtitan shanshanesis*, the finger-like epipophysis is present on the postzygapophysis, whereas this feature is absent in *Chuanjiesaurus anaensis*).

Mamenchisaurus jingyanensis

Mamenchisaurus jingyanensis (Zhang et al. 1998) is from the Late Jurassic Upper Shaximiao Formation of Sichuan. The paratype includes three cervical vertebrae, but only Cv 5 is completely preserved. Cv 5 of *Mamenchisaurus jingyanensis* bears well-developed lateral pneumatic fossae as in *Xinjiangtitan shanshanesis*, but the cervical vertebrae of *Mamenchisaurus jingyanensis* lack ventral keels, unlike *Xinjiangtitan shanshanesis*. The complex laminae and fossa are present in the whole cervical series in *Xinjiangtitan shanshanesis*, whereas the cervicals of *Mamenchisaurus jingyanensis* are poorly preserved and the description in original paper is too simple for further comparations

Klamelisaurus gobiensis

Klamelisaurus gobiensis (Zhao 1993; Moore et al. 2017) was named by Zhao in 1993. The holotype, IVPP V9492, was found in the Shishugou Formation. Unlike *Xinjiangtitan shanshanesis*, the neck of *Klamelisaurus gobiensis* includes 16 cervicals (Zhao 1993) (vs.18 cervicals in *Xinjiangtitan shanshanesis*); the ventral surfaces of the cervical centra in *Klamelisaurus gobiensis* are flat and lack keels (vs. concave and ventrally keeled cervical centra in *Xinjiangtitan shanshanesis*); and the longest cervical is Cv11 (470 mm) in *Klamelisaurus gobiensis*, while the longest cervical of *Xinjiangtitan shanshanesis* is Cv 12 (1230 mm). Finally, only the last cervical neural spine of *Xinjiangtitan shanshanesis* is bifurcated (whereas the last three cervical neural spines of *Klamelisaurus gobiensis* are bifurcated).

Euhelopus zdanskyi

Euhelopus zdanskyi was excavated from the Mengyin Formation in Shandong Province (Wiman 1929; Wilson and Upchurch 2009). According to the redescription of the cranial and postcranial anatomy of *Euhelopus zdanskyi* (Wilson and Upchurch 2009), the 'bifurcated' neural spine of the cervical is similar to the condition in *Xinjiangtitan shanshanesis*, and herein we would compare these two taxa.

As in *Euhelopus zdanskyi* (Wilson and Upchurch 2009), the centrum of the axis of *Xinjiangtitan shanshanesis* is pinched at midlength and bears expanded anterior and posterior ends; the ventrolateral ridge extends along the ventrolateral margin of the centrum in the postaxial cervical vertebrae; an oblique ridge subdivides the lateral pleurocoel. But differently, by Cv 17 (the last one) the pleurocoel is a deep pit without the oblique ridge in *Euhelopus zdanskyi* (vs. by Cv 17 pleurocoel is a deep pit with a horizontal ridge in *Xinjiangtitan shanshanesis*). Unlike *Xinjiangtitan shanshanesis*, the neck of *Euhelopus zdanskyi* includes 17 (Wilson and Upchurch 2009) cervicals (vs.18 cervicals in *Xinjiangtitan shanshanesis*); the axial centrum of *Xinjiangtitan shanshanesis* bears a longitudinal fossa on both sides of the ventral surface, and the postzygapohysis of the axis does not extend beyond the posterior margin of the centrum; *Xinjiangtitan shanshanesis* lacks the small notch on the dorsal margin of the posterior articular surface of the cervical centrum which is present in *Euhelopus zdanskyi*. The cervical neural arch of *Euhelopus zdanskyi* has an accessory lamina, which runs from the PODL up to the SPRL, but this lamina is absent in *Xinjiangtitan shanshanesis*. In *Xinjiangtitan shanshanesis*, the cervical neural spine bifurcates with paired metapophyses and a median tubercle, but the median tubercle develops as a small projection that is much lower than the posterolaterally projected metapophyses (vs. the well-developed finger-like median tubercle as tall as the metapophyses in *Euhelopus zdanskyi*). Furthermore, the neural spine of *Xinjiangtitan shanshanesis* is bifurcated only in the last cervical (vs. from Cv 12 onwards, the neural spine is subtly bifurcated in *Euhelopus zdanskyi*).

Based on comparisons with other mamenchisaurids, we are inclined to assign *Xinjiangtitan shanshanesis* in the

Mamenchisauridae, and it is possibly closely related to *Qijianglong guokr*. In both *Xinjiangtitan shanshanesis* and *Qijianglong guokr*, the number of the cervical vertebrae is more than 16; the cervical centra bear internal pneumaticity; the lateral pneumatic fossa present on the centrum which is divided by a bony septum, defining an anterior and a posterior lateral excavation; the ventral surface of the cervical centra is transversely concave and the ventral keel is present as a low ridge; the small notch in the dorsal margin of the posterior articular surface of cervical centra is absent; the neural spine is low and the neural spine of posterior cervical vertebrae is bifid; a subtle keel subdivides the spinodiapophyseal fossa in the middle-posterior cervical vertebrae in *Xinjiangtitan shanshanesis*, and in Cv 16 and Cv 17 in *Qijianglong guokr*; pneumatopores exist in the spinodiapophyseal fossae in the middle-posterior cervical vertebrae; the finger-like epipophysis is situated above the postzygapophysis in Cv 7 -Cv 14 in *Xinjiangtitan shanshanesis* and in Cv 5 -Cv 14 in *Qijianglong guokr*.

Despite these similarities, *Xinjiangtitan shanshanesis* also possesses some features that distinguish it from other known mamenchisaurids, such as the ventral keel present on the postaxial cervicals (at various positions along the column), the last cervical neural spine bifurcated with median metapophyses, the articular surface of the prezygapophysis weakly convex, the CPRL of Cv 18 dorsally divided and connecting to the prezygapophysis, the height to width ratio of the posterior articular surface of the cervical centrum greater than 1.1, and perhaps the neck being the longest among the mamenchisaurids that have been reported so far. The taxonomic position of *Xinjiangtitan shanshanesis* awaits careful examination with additional materials and further phylogenetic analyses.

Acknowledgments

We thank the Shanshan Geological Museum, and Gansu Sinian Dinosaur Culture Communication Co. Ltd for their field assistance and the preparation of the specimen. We thank the Gansu Geological Museum, the Key Laboratory of Vertebrate Evolution and Human Origins of Chinese Academy of Sciences, the Institute of Vertebrate Paleontology and Paleoanthropology, Chinese Academy of Sciences for supporting this research. We would also like to thank Dr Lü Junchang, Zhou Linqi, Wang Yaming, Yang Jingtao, Li Longfeng and Zhang Qiannan for all of their assistance. Fieldwork funding was provided by the Rescue Excavation Project of Dinosaur Fossils in Shanshan, Xinjiang. HLY is supported by the Strategic Priority Research Program of Chinese Academy of Sciences (XDB26000000) and the National Natural Science Foundation of China (Grants No. 41688103, 41872021 and 41472020).

Disclosure statement

No potential conflict of interest was reported by the authors.

Funding

This work was supported by the Scientific Innovative Fund of Gansu Agricultural University [Nos 066-056001].

ORCID

Hai-Lu You http://orcid.org/0000-0003-2203-6461

References

Bohlin B. 1953. The Sino-Swedish Expedition Publication 37, □. Vertebrate Palaeontology 6: Fossil Reptiles from Mongolia and Kansu (Statens Etnografiska Museum).

Deng SH, Wang SE, Yang ZY, Lu ZY, Li X, Hu QY, An CZ, Xi DP, Wan XQ. 2015. Comprehensive study of the middle-upper jurassic strata in the junggar basin, Xinjiang. Acta Geosci Sin. 36(5):559–574.

Dong ZM. 1990. On remains of the sauropods from Kelameili region, Junggar Basin, Xinjiang, China. Vertebrata PalAsiatica. 28(1):43-58.

Dong ZM. 1997. A gigantic sauropod (*Hudiesaurus sinojapanorum* gen. et sp. nov.) from the Turpan Basin, China. In: Dong ZM, editor. Sino-Japanese Silk Road Dinosaur Expedition. Beijing: China Ocean Press; p. 102-110.

Fang XS, Pang QQ, Lu LW, Zhang ZX, Pan SG, Wang YM, Li XK, Cheng ZW. 2000. Lower, middle, and upper jurassic subdivision in the Lufeng region, Yunnan Province. In: Editorial Committee of the Proceedings of the Third National Stratigraphical Congress of China, editor. Proceedings of the third national stratigraphical congress of China. Beijing: Geological Publishing House; p. 208–214. [in Chinese].

Gilmore CW. 1936. Osteology of *Apatosaurus*, with special reference to specimens in the Carnegie museum. Mem Carnegie Mus. 11:175–271.

Harris JD. 2006. The axial skeleton of the dinosaur *Suuwassea emilieae* (Sauropoda: flagellicaudata) from the upper jurassic morrison formation of Montana, USA. Palaeontology. 49:1091–1121.

Hatcher JB. 1901. Diplodocus (Marsh): its osteology,taxonomy, and probable habits, with a restoration of the skeleton. Mem Carnegie Mus. 1:1–63.

He XL, Li K, Cai KJ. 1988. Sauropod dinosaur (2) *Omeisaurus tianfuensis*. the middle jurassic dinosaurian fauna from dashanpu, Zigong, Sichuan 4. Chengdu: Sichuan Publishing House of Science and Technology; p. 1–143.

He XL, Yang SH, Cai KJ, Li K, Liu ZW. 1996. A new species of sauropod, *Mamenchisaurus anyuensis* sp. nov. In: Papers on geosciences contributed to the 30th international geological congress. Chengdu (China): Chengdu University of Technology; p. 83–86.

Li K. 1998. The sauropoda fossils and their stratigraphical distribution in China. J Chendu Univ Technol. 25(1):59–60. [in Chinese].

Moore A, Clark J, Xu X. 2017. T1 – ABSTRACT: anatomy and systematics of *Klamelisaurus gobiensis*, a mamenchisaurid sauropod from the middle-late jurassic shishugou formation of China. Program and Anstracts of Annual Meeting of the Society of Vertebrate Paleontology. 165-166. doi:10.13140/RG.2.2.14403.30245

Ouyang H, Ye Y. 2002. The first mamenchisaurian skeleton with complete skull, *Mamenchisaurus youngi*. Chengdu: Sichuan Publishing House of Science and Technology; p. 1–111.

Russell DA, Zheng Z. 1993. A large mamenchisaurid from the Junggar Basin, Xinjiang, People Republic of China. Can J Earth Sci. 30:2082–2095.

Sekiya T. 2011. Re-examination of *Chuanjiesaurus anaensis* (Dinosauria: sauropoda) from the middle jurassic chuanjie formation, Lufeng County, Yunnan Province, southwest China. Mem Fukui Prefectural Dinosaur Mus. 10:1–54.

Tang F, Jin XS, Kang XM,Zhang GJ. 2001. *Omeisaurus maoianus*□A Complete Sauropoda from Jingyan, Sichuan. Beijing: China Ocean Press. P. 128.

Wilson JA. 1999. A nomenclature for vertebral laminae in sauropod dinosaurs and other saurischian dinosaurs. J Vertebr Paleontol. 19:639–653.

Wilson JA. 2012. New vertebral laminae and patterns of serial variation in vertebral laminae of Sauropod Dinosaurs. Mus Paleontol Univ Mich. 32:91–110.

Wilson JA, D'Emic MD, Ikejiri T, Moacdieh EM, Whitlock JA, Farke A. 2011. A nomenclature for vertebral fossae in Sauropod dinosaurs and other saurischian dinosaurs. PLoS One. 6(2):e17114.

Wilson JA, Upchurch P. 2009. Redescription and reassessment of the phylogenetic affinities of *Euhelopus zdanskyi* (Dinosauria: sauropoda) from the early cretaceous of China. J Syst Palaeontol. 7:199–239.

Wiman C. 1929. Die Kriede-dinosaurier aus Shantung. Palaeontol Sin Ser C. 6:1–67.

Wu WH, Zhou CF, Oliver W, Sekiya T, Dong ZM. 2013. A new gigantic sauropod dinosaur from the middle jurassic of shanshan, Xinjiang. Global Geol. 32:437–446. [in Chinese].

Xing LD, Miyashita T, Zhang JP, Li DQ, Ye Y, Sekiya T, Wang FP, Currie PJ. 2015. A new sauropod dinosaur from the late jurassic of China and the diversity, distribution, and relationships of mamenchisaurids. J Vertebr Paleontol. 35(1):e889701.

Xu JR, Li K, Liu J,Yang CY. 2014. Evaluation of dinosaur fossil resources in China. Scientific and Technological Management of Land and Resources. 31(2):8–16.

Yang ZJ, Zhao XJ. 1972. *Mamenchisaurus hochuanensis*. Inst of Vertebr Paleontol Paleoanthropology Monogr Ser I. 8:1–30. [in Chinese].

Young CC. 1937. A new dinosaurian from Sinkiang. Palaeontologia Sinica, New Ser. C, Whole Ser. 105: 1–29.

Young CC. 1954. On a new sauropod from yiping, szechuan, China. Sci China Ser A. 3(4):142–155+196.

Young CC. 1958. New sauropod dinosaurs from China. Vertebr PalAsiatica. 2:1–29.

Zhang YH. 1988. The middle jurassic dinosaur fauna from dashanpu, Zigong, Sichuan. Sauropod Dinosaur (1). *Shunosaurus*. Vol. III. Chengdu: Sichuan Publishing House of Science and Technology; p. 89.

Zhang YH, Li KZeng QH. 1998. A new species of sauropod from the Late Jurassic of the Sichuan Basin (*Mamenchisaurus jingyanensis* sp. nov.). Journal of Chengdu University of Technology. 25(1): 61–70.

Zhao XJ. 1993. A new mid-Jurassic sauropod (*Klamelisaurus gobiensis* gen.et sp. nov.) from Xinjiang China. Vertebr PalAsiatica. 31(2):132–138. [in Chinese].